ISSN 1814-4225 (print)
ISSN 2663-2012 (online)

UDC 536.2, 539.3

doi: 10.32620/reks.2026.1.15

Oleksii NIKOLAEV, Alina KRAINYCHENKO, Mariia SKITSKA

National Aerospace University "Kharkiv Aviation Institute", Kharkiv, Ukraine

MATHEMATICAL MODELING OF THE THERMAL STRESS STATE OF A BALL WITH AN ECCENTRIC HEAT-ACTIVE SPHERICAL INCLUSION

Today, technical systems with internal heat generation are developed and used in various areas of industry, energy, construction, as well as in microelectronics, nanotechnology, biomedicine, technical chemistry, ecology, etc. The creation of such systems is usually preceded by their mathematical and computer modeling, in which issues of strength often play a primary role. The use of purely numerical methods for this purpose does not always give results of the required accuracy, and the impossibility of parametric description of the model does not allow solving optimization problems with them. Therefore, the creation of new methods for modeling such systems and their models is an ***actual scientific and practical task***. ***The subject of the research*** *of the present article is mathematical models of the thermoelastic state of a ball with a spherical inclusion having a heat release region, as well as methods for obtaining them.* ***The goal of the study*** *is to create a number of parametric models for studying temperature fields and stress fields in a piecewise homogeneous sphere with an internal heat-active region under different thermomechanical conditions on its boundary. To achieve this goal, it is necessary to solve a* ***number of problems****: to perform further development of the generalized Fourier method for the class of axisymmetric stationary thermoelastic problems for a ball with an eccentric heat-active spherical inclusion, using the developed method, obtain a number of models of the thermoelastic state of a ball in cases of eccentric and concentric inclusions with a certain area of heat generation in them, perform a rigorous justification of the proposed approach, conduct a wide computer experiment with the constructed models and an analysis of the thermomechanical characteristics obtained with its help, and draw conclusions based on the results of the study.* ***The modeling methods*** *used in this work are the generalized and ordinary Fourier methods.* ***The following results*** *were obtained in the work. A number of mathematical models of the axisymmetric stationary thermoelastic state of a ball with a spherical inclusion were constructed under the condition that the entire inclusion or part of it releases heat according to a harmonic law. The cases of a stationary surface of a ball and a constant temperature on its boundary, as well as a ball whose surface is loaded with normal pressure and is in conditions of heat exchange with the environment are considered. Modeling is carried out using the generalized Fourier method, which was further developed in the work. Determination of the parameters of the models is reduced to solving infinite systems of linear algebraic equations. For the two specified types of models, the case of concentric inclusion is considered separately. Linear algebraic systems of the fourth order are obtained to determine the parameters of the models. Using a new classical inequality, lower bounds for the moduli of the determinants of systems and the existence classes of the resulting models were obtained for the first time. Separately, a thermoelastic model of a ball with a spherical thermally active layer in the inclusion was obtained in a closed form. Different types of ball and inclusion materials were used in the numerical simulation. Calculations were performed for temperature fields and stress fields with changes in geometric parameters, values and density functions of heat sources. Rich graphic material was obtained and analyzed in the work.* ***Scientific novelty****: all the above results are new. Conclusions were made based on the results of the studies.*

Keywords: *mathematical model; sphere with heat-active inclusion; generalized Fourier method; temperature and stress fields; density of heat sources; thermomechanical characteristics; eccentric inclusion; computer simulations; lower bound of the determinant module.*

1. Introduction

1.1. Motivation

Many problems of modern engineering are related to natural or artificial objects, which, in addition to thermal deformation effects from the environment, also have internal heat sources localized on certain surfaces or in volumes inside the bodies. Such objects include, for example, heat generators, industrial furnaces, underfloor heating systems, multilayer microcircuits, underground storage facilities, geothermal reservoirs, as well as elements that generate heat in nuclear density engineering.

A separate group consists of spherical structures with internal heat sources used in nanotechnology. Nanoparticles with a core-shell architecture or in the form of nano capsules are used in such areas as biomedicine (for example, for point heating of tumors), energy (as battery components), technical chemistry (localized catalysis), ecology (decomposition of organic pollutants) and others.

Mathematical modeling of such systems requires taking into account the density distribution, shape and location of heat sources, which significantly complicates the calculations. At the same time, existing numerical and analytical-numerical methods often do not provide the required accuracy and completeness of results and, in addition, often require large computational resources. Therefore, the development of effective approaches to solving boundary problems of thermoelasticity taking into account complex geometry, as well as various thermal and mechanical factors, remains an actual problem today.

Research into spatial problems of elasticity theory for a sphere and a space with a spherical cavity goes back to the works of the classics of natural science and began in the mid-19th century. It is believed that the problem of an elastic sphere was first considered by G. Lame in his treatise [1]. In it, problems of vibration of a solid sphere and constant normal pressure on a hollow sphere were investigated. This work laid the foundations for modern methods of solving similar problems: the Lame equation was written in spherical coordinates, and with the help of a potential function, this equation was transformed into a wave equation, to which the method of separation of variables was applied. In constructing solutions, series of functions, some analogues of Legendre functions, were used. The second work devoted to the hollow sphere belongs to W. Thomson [2] and appeared more than ten years after Lame's lectures. In it, the problem is considered in a general formulation. The solution is presented in the form of density series in the radial coordinate with coefficients containing combinations of surface spherical harmonics (expressed in Cartesian coordinates). After substituting into the equation of equilibrium in displacements, a system of differential equations is obtained for these harmonics on the surfaces of the sphere. In the work of C. Somigliana [3], problems are investigated for a solid sphere, a space with a cavity, and a sphere with an internal cavity with given displacements on concentric surfaces. The displacements are expressed through combinations of volume and surface potentials. The problems are then broken down into simpler ones, the solutions of which can be reduced to calculating one-dimensional integrals. In the case of a hollow sphere, the solutions are presented in the form of single series with difficult-to-calculate terms. The article [4] is devoted to the solution of the problem for a hollow sphere with symmetrical loading on its surfaces. Here the displacements are expressed through surface potentials in the form of series similar to those used to specify the generating function of Legendre polynomials. Various formulations of problems for elastic solid and hollow spheres are considered in the monograph [5]. The solutions are constructed in the form of series in spherical functions. Apparently, the case of concentrated forces acting on an elastic sphere was first analyzed in [6]. The solution is decomposed into two groups of terms: the first describes special solutions obtained as limits from a uniformly distributed load near the poles of the sphere; the second is the standard series of spherical functions. As for the problem of a spherical inclusion in an infinite elastic body, apparently one of the first such studies was carried out in work [7], where solutions in the form of series in spherical functions were used to analyze the influence of a small inclusion on the disturbance of a homogeneous stress state in the body.

Let us consider the state of modern research in the field of thermoelasticity of canonical bodies. Their authors, first of all, develop analytical-numerical methods for solving this class of problems.

1.2. State of the art

In the work [8] simple types of loading of an infinite matrix with spherical heterogeneity are considered: constant uniaxial and triaxial loads. An inclusion or a cavity is selected as the heterogeneity. Solutions to the problems are obtained by elementary methods. The displacement of the points of the heterogeneity surface is specified through the displacement of the points of the poles and the equator, directly expressed through the external load. The connection between the displacements of the specified points and the stresses on the boundary of the heterogeneity is carried out by the method of compatibility of deformations for statically indeterminate systems. The paper [9] considers the problem of displacement and rotation of a weakly deformed spherical rigid inclusion embedded in an unbounded elastic medium. The inclusion surface is described as a perturbed spherical surface using a term having the first order of the small parameter. The boundary condition for the displacement vector is set on the perturbed surface and includes the translation vector and the rotation vector. Series in tensor spherical functions and asymptotic series in the small parameter are used. The problem is divided into two separate problems for translations and rotations. The paper [10] is devoted to the analysis of the influence of interphase stresses on the elastic field inside a nanoscale inclusion. The problem is considered in a symmetric formulation. The Goodier's approach to constructing solutions to the Lame equation through two volume spherical functions is used. The displacement field in the matrix and inclusion is constructed explicitly under the condition that the auxiliary harmonic functions are chosen in the simplest form - one or two harmonics. A similar approach in the paper [11] solves the problem of the stress state of an elastic medium with a small spherical cavity. The paper [12] presents a closed-form solution for stress fields around a rigid spherical nanoparticle under uniaxial tensile loading. The work explicitly takes into account the presence of an interphase surface around the nanoparticles with a thickness comparable to the particle size and elastic properties

 ISSN 1814-4225 (print)
ISSN 2663-2012 (online)

different from those of the matrix. Only the principal terms of displacements and stresses in the matrix and the interphase spherical layer are taken into account. In [13], the stress field in an infinite body with a spherical inclusion surrounded by a spherical layer embedded in an infinite matrix is investigated. The entire body is subjected to a uniform load at infinity. The approach used consists of directly solving the Lame equation separately for the deviatoric and hydrostatic parts of the deformations in the infinitely distant region. It is assumed that the displacement has a form directly proportional to the specified deformations, with unknown functions that have yet to be determined. Differential equations are obtained with respect to the functions, which are solved analytically. The results are obtained in closed form.

The application of analytical and numerical methods in the study of stationary thermal and thermoelastic fields is typical for plane problems and spatial problems in canonical domains. In [14], under the action of a stationary heat source, the Boussinesq functions of the thermoelasticity problem for plane deformation of a semi-infinite body with a free, rigid, smooth or flexibly fixed boundary on which zero temperature or thermal insulation is maintained are constructed. The construction of the Boussinesq functions is reduced to solving boundary value problems for harmonic functions in a half-space. A relation is obtained for displacements and stresses, which are the corresponding Green's functions and can be used to determine the thermoelastic state of a half-space based on heat release in a tape domain. In [15], when solving a stationary thermoelastic problem for an isotropic cylinder of finite length, the temperature field was divided into two components: symmetric and antisymmetric relative to the axial coordinate of the cylinder. In each case, the temperature field is sought in the form of a Fourier series along the axial coordinate. With respect to the radial coordinate, the solutions are expanded into Bessel-Dini series. After satisfying the boundary conditions, an infinite system of linear algebraic equations is obtained, which is solved by the improved reduction method. In the work [16] a method for determining the thermoelastic state in multilayer bodies was developed taking into account thermal factors and physical and mechanical characteristics of the material under the action of heat sources. The Kirchhoff transformation, Newton's iterative method, generalized functions and Green's functions are used to solve the problems. In the article [17] analytical solutions of the problems of stationary thermal conductivity and thermoelasticity for a semi-infinite layer are obtained under conditions of smooth contact at the end. The solution method is based on reducing the Lame equations to two jointly solved equations and one equation that is solved separately. The equations are exactly solved by the method of integral transformations. The author [18] considered thermal stresses caused by the difference in the coefficients of thermal expansion of a spherical inclusion and a matrix. It is assumed that the inclusion and matrix have cubic symmetry. The Eshelby equivalent inclusion method is used to solve the problem. In the work [19], using general Love solutions, the authors construct solutions to boundary value problems for an elastic and thermoelastic space with a spherical inclusion or cavity.

In a number of studies, finite and boundary element methods and their modifications are used to solve thermoelastic problems. The authors of the article [20] applied a known solution for a constant temperature distribution in a rectangle together with the method of boundary integral equations to obtain an approximate solution of a plane stationary thermoelastic problem with mixed mechanical boundary conditions. Unknown functions in the section are obtained in the form of series in Cartesian harmonics and additional harmonic functions that have singularities at the points of change of boundary conditions. Another approach is demonstrated in the article [21], where, to implement the boundary element method in three-dimensional thermoelasticity problems, the transformation of the triple integral associated with the temperature field into a surface integral in the boundary integral equation is carried out using the Green’s function.

Some studies investigate internal heat sources. In the article [22] a stationary thermal field in a solid sphere with constant density of heat sources is investigated. The cases of constant thermal conductivity of the sphere and linearly dependent on temperature are considered. In both cases the heat conductivity equation, depending only on the radial coordinate, is simply integrated in closed form. The paper [23] considers a method for solving axisymmetric problems of stationary thermal conductivity and thermoelasticity for a body with a thin heat-active inclusion. Localized thin flat inhomogeneities are modeled by a sheet of heat sources located in the plane of an unbounded body and specified by the Hankel transformation with respect to the radial variable of some parametric generating function. The stress-strain state of the entire body is represented in a similar way. The solution to the problem is obtained after transforming a singular integral equation with a Bessel kernel using discontinuous Weber–Schaffheitlin integrals into an expansion of a given function in a series in terms of a system of orthogonal Jacobi polynomials. The article [24] is devoted to the determination of the temperature field and stress state of an unlimited body with one heat-generating spherical inclusion at different thermophysical and mechanical parameters, as well as with a system of spherical thermal inclusions. Thermal inclusions are understood as inclusions whose materials have elastic properties identical to the elastic properties of the matrix material. In this case, only the coefficients of thermal conductivity and linear thermal expansion are different. The density of the sources is also constant. For one inclusion, an exact solution of the problem is obtained through the fundamental solution of the Laplace equation. For a system of inclusions, the solution is actually obtained by the method of superposition of the previous solution with potentials associated with the centers of the inclusions. In [25], the Boussinesq functions of stationary thermoelasticity problems for a half-space with a free, rigid, smooth or flexibly fixed boundary at zero temperature or thermal insulation on it and the action of a heat-generating thermal spherical inclusion are constructed. Thermoelastic displacement potentials in space with two spherical inclusions are used to construct these functions. The problem for a thermal inclusion is considered. The solution of the problem for one inclusion (the density of the sources is constant) in an elastic space and the method of symmetric or antisymmetric continuation through the boundary of the half-space (the image method) are used. In [26], the steady-state thermoelastic state of a hollow sphere made of a functionally graded material is investigated. All thermomechanical characteristics are considered variables that change according to density laws depending on the radial variable. The relationship between stresses and strains is carried out according to Hooke's law, which takes into account thermal strains. Since all unknown functions in the problem under consideration depend only on the radial coordinate, the heat conduction and equilibrium equations are integrated in closed form. In a similar manner, in [27], the thermoelastic state of a hollow cylinder made of a functionally graded material is determined. The article [28] considers a multilayer sphere with heat sources in each layer, the densities of which are constant. The thermal field in each layer is determined separately and depends only on the radial coordinate and time. The conditions of ideal thermal contact are satisfied on the surfaces of the layers. The stresses are associated with the Hook's law deformations taking into account thermal expansion. The equilibrium equations in stresses are directly integrated for each layer. The thermal field in the layer is divided into two components: one is responsible for the transient process, the other for the stationary temperature distribution. For the n layers, the problem is reduced to solving multiparameter systems of order $2n$, the solvability analysis of which is not given. In paper [29], a transient thermal process occurring in a composite with spherical inhomogeneities under the influence of a short-term laser pulse is investigated. Modeling of thermal fields in the space-time domain is carried out by a combination of two approaches: the Eshelby method, which takes into account the eigen fields in inclusions, and the boundary element method, which takes into account boundary effects. In the particular case of a composite disk, parametric modeling is carried out with different ratios of disk thickness and particle size. A similar approach applied to another problem was implemented in [30], which considered a unit cubic matrix with ellipsoidal inclusions. The article investigated the thermoelastic properties of composites and the effect of particle parameters on them. The presence of particles was modeled by the equivalent inclusion method, according to which the effect of heterogeneity of the matrix and inclusion materials was taken into account by the proper deformations and temperature gradient. Boundary conditions were satisfied using an integral equation solved by the boundary element method. A separate model was developed with spherical particles randomly distributed in a unit cube. The model was used to study the effect of particle volume fractions and their materials on the effective properties of the composite. The paper [31] studies the thermomechanical characteristics of two-phase composites with architectural design of various topologies. The topology is taken into account using the Gielis' formula. Effective thermal conductivity coefficients and elastic moduli in a wide range of elastic and thermal parameters of phase attributes are estimated based on the Galerkin boundary element method. The feature space includes, along with thermomechanical characteristics, the volume fraction of phases and their geometric design. The feature space is used to train deep neural networks. The latter are used to analyze the dependencies between the basic parameters and interpret the results using the Shapley algorithm. In the article [32] two-dimensional uncoupled stationary problems of heat conduction and thermoelasticity for an infinite matrix imperfectly coupled to an elliptical isotropic elastic heterogeneity are considered. A uniform remote heat flux and a uniform temperature change are applied to the matrix. The imperfect coupling of the matrix and the heterogeneity is due to the weak heat conductivity and the spring connection between the matrix and the heterogeneity and is modeled by two interface functions. The problem is reduced to such a choice of interface functions that the uniform heat flux causes a linear stress distribution, and a constant temperature change causes a constant stress distribution in the heterogeneity. As a result, the temperature and stress fields in the matrix and heterogeneity are obtained in closed form. In article [33], a hierarchical multiscale model of the influence of thermal stresses on the viscous failure of polymer composites with nanoparticles is developed. In the model, the failure process is associated with the detachment of nanoparticles. A representative element of a polymer with a spherical nanoparticle and an interphase region filled with a certain material were considered. Calculations based on the constructed model and confirmed experimentally showed a significant effect of temperature on viscous failure caused by the failure mechanism. The model made it possible to relate thermomechanical characteristics such as: mass fraction of nanoparticles, coefficient of thermal expansion, thickness, Young's modulus with the parameters of viscous failure. The importance of

ISSN 1814-4225 (print)
ISSN 2663-2012 (online)

constructing parametric models of the thermoelastic state of composite multi-connected bodies can be traced in the article [34], which proposed a method for solving optimal control problems based on similar models. Articles [34, 35] are based on the application of the generalized Fourier method. The spherical solutions of the Lamé equation used in them are constructed as basis vector solutions, which distinguishes them from the solutions of Goodier, Love, Lure, and others. In the monograph [36], the author used the apparatus of tensor solutions to the equations of elasticity and thermoelasticity theory, the tensor Green's function, and the Eshelby method to account for inhomogeneities to study a wide range of problems in the micromechanics of inhomogeneous materials. An approach similar to that presented in the article [11] was used to construct the Eshelby tensor for a spherical inhomogeneity. The case of an ellipsoidal inclusion is considered in more detail. To implement the interface conditions, the method of fundamental solutions and boundary integral equations was used. Problems with random inclusion characteristics were also considered.

The above bibliographic review allows us to draw the following conclusions:

1. In scientific periodicals, there are no studies of the first and second boundary value problems of the theory of elasticity and thermoelasticity in a general axisymmetric formulation for a sphere with a concentric or eccentric spherical inclusion, taking into account heat generation or without it.

2. The proposed solutions to the problems considered in the articles (except for trivial ones) are heuristic in nature, since they practically do not include elements of justification.

1.3. Objectives and tasks

In connection with the above, the purpose of this work is the further development of the apparatus of the generalized Fourier method for axisymmetric stationary thermoelastic problems for multi-connected spatial domains bounded by spherical surfaces; the use of the developed apparatus for modeling the thermoelastic state of a sphere with an eccentric spherical inclusion that releases heat according to a harmonic law; rigorous justification of the constructed models.

To achieve the set goals, it is necessary to solve the following tasks:

1. To perform further development of the generalized Fourier method for the class of axisymmetric stationary thermoelastic problems for a ball with an eccentric heat-active spherical inclusion

2. Construct parametric models of the thermoelastic state of a ball with an eccentric spherical inclusion that releases heat according to a harmonic law, under general axisymmetric boundary conditions of the first and second kind on the surface of the sphere.

3. Perform a rigorous mathematical justification of the constructed models.

4. Consider separately the limiting case of a concentric inclusion.

5. Obtain an accurate closed-form model of the thermoelastic state of a sphere with a concentric inclusion having a heat-active spherical layer.

6. Conduct a computer simulation with the constructed models.

7. To draw conclusions based on the research results.

The article is structured as follows.

Section 1 provides an introduction to the study. Section 1.1 discusses the motivation for this study and provides arguments for the relevance of the chosen topic. A historical overview of the works of classic natural scientists devoted to this topic is provided. Section 1.2 provides a bibliographic review of recent research on related topics. Based on the review's findings, Section 1.3 formulates the study's objectives and sets the tasks that should lead to their achievement. This section also outlines the structure of this article.

Section 2 presents the mathematical formulation of the modeling problem.

Section 3 constructs a model of a stationary axisymmetric temperature field for a sphere with an eccentric spherical inclusion that generates heat harmonically at a given temperature on the sphere's surface. A theorem is proved that validates the correctness of the model.

Section 4 constructs a model of the thermoelastic state of a fixed composite sphere subject to the temperature field described in Section 3. The modeling is performed using the generalized Fourier method, which is further developed in this section. Theorem 3 substantiates the correctness of the constructed model.

Section 5 separately constructs the model from the previous section for the case of a concentric spherical inclusion. The problem of justifying such a model is considered, the solution to which is based on the results of Theorem 4. The existence condition for the model is given in Theorem 5.

Section 6 constructs models of the temperature field and thermoelastic state of a loaded sphere with an eccentric spherical inclusion that generates heat, assuming heat exchange between the sphere's surface and the surrounding medium. The correctness of the model is substantiated by Theorem 6.

In Sections 7 and 8, models of the temperature field and thermoelastic state of a loaded sphere are constructed for cases of a fully or partially thermally active concentric spherical inclusion. The condition for the existence of the model is laid down in Theorem 7.

Section 9 presents the results of computer simulation and their analysis for all constructed parametric models.

Section 10 discusses the results of the study and points out the need for a controlled selection of the physical and mechanical parameters of the models to meet the elasticity conditions.

Section 11 presents conclusions based on the research findings: the relevance of the topic, the solution to the stated problems, the scientific novelty, reliability, and practical significance of the results obtained. The advantages of the proposed modeling method over existing methods are highlighted.

2. Mathematical statement of the problem

Consider an elastic ball $B_{R_1}(O_1)$ centered at a point O_1 of radius R_1, which has an eccentric spherical elastic inclusion $B_{R_2}(O_2)$ centered at a point O_2 of radius R_2 ($|O_1O_2|+R_2<R_1$) made of another material. Let us introduce two spherical coordinate systems (r_j,θ_j,φ) ($j=1,2$), the origins of which are aligned with the points O_j ($|\overrightarrow{O_1O_2}|=z_{12}$), and their axes of symmetry have the direction of the vector $\overrightarrow{O_1O_2}$. Let us denote the domains $\Omega_1=B_{R_1}(O_1)\setminus\overline{B_{R_2}(O_2)}$, $\Omega_2=B_{R_2}(O_2)$. We will assume that the material of the part of the sphere that occupies the domain Ω_j has thermomechanical characteristics (G_j,ν_j,α_j,k_j) ($j=1,2$), where G is the shear modulus, ν is the Poisson's ratio, α is the coefficient of linear thermal expansion, k is the coefficient of thermal conductivity.

At first, we will construct a parametric model of the thermally stressed state of a ball $B_{R_1}(O_1)$, the surface Γ_1 of which is fixed and is at zero temperature. We assume that the conditions of ideal thermomechanical contact are fulfilled on the surface Γ_2 of the inclusion, and the inclusion itself releases heat with a density $k_2 g(r_2,\theta_2)$. We note that homogeneous thermomechanical conditions on the surface Γ_1 do not limit the generality of the model that will be constructed.

The mathematical model of the thermally stressed state of the system under consideration is a boundary value problem for a system of elliptic partial differential equations ($j=1,2$)

$$\vec{\nabla}^2\vec{U}_j+\frac{1}{1-2\nu_j}\vec{\nabla}(\vec{\nabla}\vec{U}_j)=\alpha_j\frac{2+2\nu_j}{1-2\nu_j}\vec{\nabla}T_j,\quad \vec{x}\in\Omega_j;\qquad(1)$$

$$\vec{\nabla}^2 T_j+\delta_{j,2}g=0,\quad \vec{x}\in\Omega_j\qquad(2)$$

with boundary conditions

$$(T_1)_{|\Gamma_1}=T_0,\qquad(3)$$

$$(\vec{U}_1)_{|\Gamma_1}=0\qquad(4)$$

and the conditions of conjugation of thermomechanical fields

$$(T_1)_{|\Gamma_2}=(T_2)_{|\Gamma_2},\quad \left(k_1\frac{\partial T_1}{\partial n_2}\right)_{|\Gamma_2}=\left(k_2\frac{\partial T_2}{\partial n_2}\right)_{|\Gamma_2};\qquad(5)$$

$$(\vec{U}_1)_{|\Gamma_2}=(\vec{U}_2)_{|\Gamma_2},\quad (F\vec{U}_1)_{|\Gamma_2}=(F\vec{U}_2)_{|\Gamma_2}.\qquad(6)$$

Here (T_j, $\vec{U}_j$) ($j=1,2$) denotes the temperature field and the displacement field in the domain Ω_j, $F\vec{U}_j$ is the stress vector on the surface Γ_j with the normal $\vec{n}_j=\vec{e}_{r_j}$, corresponding to the displacement vector $\vec{U}_j$, $\delta_{j,k}$ is Kronecker delta symbol, $\vec{\nabla}$ is the operator of the nabla, $\{\vec{e}_{r_j},\vec{e}_{\theta_j}\}$ are the unit vectors of the spherical coordinate system with the origin at the point O_j, $\vec{x}$ is the point of three-dimensional space, the Cartesian coordinates of which are related to the spherical coordinates by the formulas

$$x=r_1\sin\theta_1\cos\varphi_1=r_2\sin\theta_2\cos\varphi_2,$$

$$y=r_1\sin\theta_1\sin\varphi_1=r_2\sin\theta_2\sin\varphi_2,$$

$$z=r_1\cos\theta_1=z_{12}+r_2\cos\theta_2.$$

Regarding the function $g(r_2,\theta_2)$, we will assume that it is harmonic in the domain Ω_2, in the closure of which it is represented by an absolutely and uniformly convergent series

$$g(r_2,\theta_2)=\sum_{n=0}^{\infty}g_n\left(\frac{r_2}{R_2}\right)^n P_n(\cos\theta_2),\qquad(7)$$

where $P_n(x)$ is the Legendre polynomial.

3. Modeling of the temperature field

We will look for a solution to problem (2), (3), (5), (7) in the domains Ω_j in the form

$$T_1(\vec{x})=\sum_{n=0}^{\infty}t_n^{(1)}R_1^{-n}w_n^-(r_1,\theta_1)+$$

$$+\sum_{n=0}^{\infty}t_n^{(2)}R_2^{n+1}w_n^+(r_2,\theta_2),\quad \vec{x}\in\Omega_1;\qquad(8)$$

$$T_2(\vec{x})=\sum_{n=0}^{\infty}R_2^{-n}[d_n r_2^2+c_n]w_n^-(r_2,\theta_2),\quad \vec{x}\in\Omega_2\qquad(9)$$

with unknown parameters $\{t_n^{(j)}\}_{n=0,j=1}^{\infty,2}$, $\{d_n\}_{n=0}^{\infty}$,

ISSN 1814-4225 (print)
ISSN 2663-2012 (online)

$\{c_n\}_{n=0}^{\infty}$. Here the axisymmetric basis solutions of the Laplace equation for the exterior $\Omega^+ = \{r > R\}$ and interior $\Omega^- = \{r < R\}$ of the sphere are denoted by

$$w_n^{\pm}(r,\theta) = r^{\mp(n+1/2)-1/2} P_n(\cos\theta), \quad (10)$$

where the sign + (–) corresponds to the external (internal) solution.

Let us find the parameters d_n in solution (9) of Poisson's equation (2), for which we apply the Laplace operator to the function $T_2(r_2, \theta_2)$

$$\Delta T_2(r_2,\theta_2) = \sum_{n=0}^{\infty} R_2^{-n} 2(2n+3) d_n w_n^-(r_2,\theta_2) .$$

Comparing this result with (2) and (7), we obtain

$$d_n = -\frac{g_n}{2(2n+3)} . \quad (11)$$

Let's use the formulas ($n = 0 \div \infty$)

$$w_n^+(r_2,\theta_2) = \sum_{k=n}^{\infty} C_k^n z_{12}^{k-n} w_k^+(r_1,\theta_1), \; r_1 > z_{12} ; \quad (12)$$

$$w_n^-(r_1,\theta_1) = \sum_{k=0}^{n} C_n^k z_{12}^{n-k} w_k^-(r_2,\theta_2) , \quad (13)$$

where C_n^k is the binomial coefficient, that follow from the integral representations of the Legendre functions, to write the temperature field $T_1(\vec{x})$ in coordinate systems with origins at points 0_j

$$T_1(\vec{x}) = \sum_{n=0}^{\infty} t_n^{(1)} R_1^{-n} w_n^-(r_1,\theta_1) + \sum_{n=0}^{\infty} w_n^+(r_1,\theta_1) \sum_{k=0}^{n} C_n^k R_2^{k+1} z_{12}^{n-k} t_k^{(2)} , \quad (14)$$

$$T_1(\vec{x}) = \sum_{n=0}^{\infty} t_n^{(2)} R_2^{n+1} w_n^+(r_2,\theta_2) + \sum_{n=0}^{\infty} w_n^-(r_2,\theta_2) \sum_{k=n}^{\infty} C_k^n R_1^{-k} z_{12}^{k-n} t_k^{(1)} . \quad (15)$$

Satisfying the conditions of conjugation of thermal fields on the surface Γ_2 of the inclusion and the boundary condition on the surface Γ_1, we arrive at an infinite system of linear algebraic equations with respect to the unknowns $\{t_n^{(j)}\}_{n=0,j=1}^{\infty,2}$, $\{c_n\}_{n=0}^{\infty}$

$$t_n^{(1)} + \sum_{k=0}^{n} C_n^k \omega_{n+1,k+1} t_k^{(2)} = T_0 \delta_{n,0}, \; n = 0 \div \infty ; \quad (16)$$

$$t_n^{(2)} + \frac{(k_2 - k_1)n}{k_2 n + k_1(n+1)} \sum_{k=n}^{\infty} C_k^n \omega_{k,n} t_k^{(1)} = \frac{k_2 R_2^2 g_n}{(2n+3)[k_2 n + k_1(n+1)]}, \; n = 0 \div \infty ; \quad (17)$$

$$c_n = t_n^{(2)} + \sum_{k=n}^{\infty} C_k^n \omega_{k,n} t_k^{(1)} + \frac{R_2^2 g_n}{2(2n+3)}, \; n = 0 \div \infty , \quad (18)$$

where

$$\omega_{n,k} = \left(\frac{z_{12}}{R_1}\right)^n \left(\frac{R_2}{z_{12}}\right)^k .$$

The following result allows us to correctly solve system (16) – (18).

Theorem 1. The operator of the system (16), (17) is a Fredholm operator in the space l_2^2 under the condition $z_{12} + R_2 < R_1$.

Proof. To prove the theorem, it is sufficient to show the convergence of the series

$$\sum_{n=0}^{\infty} \sum_{k=0}^{n} C_n^k \omega_{n,k} = \sum_{n=0}^{\infty} \sum_{k=n}^{\infty} C_k^n \omega_{k,n} .$$

The latter follows from the condition of the theorem, since

$$\sum_{n=0}^{\infty} \sum_{k=0}^{n} C_n^k \omega_{n,k} = \sum_{n=0}^{\infty} \left(\frac{z_{12}}{R_1}\right)^n \sum_{k=0}^{n} C_n^k \left(\frac{R_2}{z_{12}}\right)^k = \sum_{n=0}^{\infty} \left(\frac{z_{12}}{R_1}\right)^n \left(1 + \frac{R_2}{z_{12}}\right)^n$$

and the last series converges as the sum of a geometric sequence with a denominator less than unity.

4. Modeling the thermoelastic state of a fixed ball

Now we will solve problem (1), (4), (6) for the temperature field, which is given by formulas (8), (9), (11), (16) – (18). For this, we will use the generalized Fourier method. In one of the previous articles of the authors, axisymmetric sets of partial solutions of the Lame equation $\{\vec{W}_{1,0}^+(r,\theta), \vec{W}_{1,n}^+(r,\theta), \vec{W}_{2,n}^+(r,\theta)\}_{n=1}^{\infty}$ ($\{\vec{W}_{2,0}^-(r,\theta), \vec{W}_{1,n}^-(r,\theta), \vec{W}_{2,n}^-(r,\theta)\}_{n=1}^{\infty}$) for the exterior Ω^+ (interior Ω^-) of the sphere were introduced and it was proved that they form systems of basis solutions in the corresponding domains $\Omega^{\pm}$. Here

$$\vec{W}_{1,n}^{\pm}(r,\theta) = \vec{\nabla} w_n^{\pm}(r,\theta) , \quad (19)$$

$$\vec{W}_{2,n}^{\pm}(r,\theta) = \chi_n^{\pm} \vec{V}_n^{\pm}(r,\theta) + \zeta_n^{\pm} \vec{W}_{1,n}^{\pm}(r,\theta) , \quad (20)$$

where

$$\vec{V}_n^{\pm}(r,\theta) = \vec{\nabla}[r^2 w_n^{\pm}(r,\theta)] , \quad (21)$$

$$\chi_n^+ = (4\nu - 3)n + 2\nu - 2, \; \zeta_n^+ = (2n-1)(2\nu - 2) , \quad (22)$$

$$\chi_n^- = (4\nu - 3)n + 2\nu - 1, \; \zeta_n^- = (2n+3)(2\nu - 2) . \quad (23)$$

In addition, we introduce the following vector functions

$$\vec{V}_n^{-(1)}(r,\theta) = \vec{\nabla}[r^4 w^-(r,\theta)] . \quad (24)$$

Next, we will use the following result [35], which is the basis of the modeling method of this article.

Theorem 2. For vector functions (19) – (21) in spherical coordinate systems with origins at points O_j, the addition theorems hold

$$\vec{W}^{+}_{1,n}(r_2,\theta_2)=\sum_{k=n}^{\infty}C_k^n z_{12}^{k-n}\vec{W}^{+}_{1,k}(r_1,\theta_1),\ r_1>z_{12},\quad n=0\div\infty; \tag{25}$$

$$\vec{W}^{+}_{2,n}(r_2,\theta_2)=\sum_{k=n}^{\infty}C_{k-1}^{n-1}\gamma^{+(2)}_{n,k}z_{12}^{k-n}\vec{W}^{+}_{2,k}(r_1,\theta_1)+\sum_{k=n-1}^{\infty}C_k^{n-1}\gamma^{+(1)}_{n,k}z_{12}^{k-n+2}\vec{W}^{+}_{1,k}(r_1,\theta_1),\ r_1>z_{12},\quad n=1\div\infty; \tag{26}$$

$$\vec{W}^{-}_{1,n}(r_1,\theta_1)=\sum_{k=0}^{n}C_n^k z_{12}^{n-k}\vec{W}^{-}_{1,k}(r_2,\theta_2),\ n=1\div\infty; \tag{27}$$

$$\vec{W}^{-}_{2,n}(r_1,\theta_1)=\sum_{k=0}^{n}C_{n+1}^{k+1}\gamma^{-(2)}_{n,k}z_{12}^{n-k}\vec{W}^{-}_{2,k}(r_2,\theta_2)+\sum_{k=0}^{n+1}C_{n+1}^{k}\gamma^{-(1)}_{n,k}z_{12}^{n-k+2}\vec{W}^{-}_{1,k}(r_2,\theta_2),\ n=0\div\infty; \tag{28}$$

$$\vec{V}^{+}_{n}(r_2,\theta_2)=\sum_{k=n}^{\infty}C_k^n\gamma^{+(2)}_{n,k}z_{12}^{k-n}\vec{V}^{+}_{k}(r_1,\theta_1)+\sum_{k=n-1}^{\infty}C_{k+1}^{n}\lambda^{+(1)}_{n,k}z_{12}^{k-n+2}\vec{W}^{+}_{1,k}(r_1,\theta_1),\ r_1>z_{12},\quad n=1\div\infty; \tag{29}$$

$$\vec{V}^{-}_{n}(r_1,\theta_1)=\sum_{k=0}^{n}C_n^k\gamma^{-(2)}_{n,k}z_{12}^{n-k}\vec{V}^{-}_{k}(r_2,\theta_2)+\sum_{k=0}^{n+1}C_{n+1}^{k}\lambda^{-(1)}_{n,k}z_{12}^{n-k+2}\vec{W}^{-}_{1,k}(r_2,\theta_2),\ n=0\div\infty, \tag{30}$$

where

$$\gamma^{+(1)}_{n,k}=\frac{k-2nk-3n+5-4\nu_1}{2k+3},\ \gamma^{+(2)}_{n,k}=\frac{2n-1}{2k-1},$$

$$\gamma^{-(1)}_{n,k}=\frac{2nk+3k-n-5+4\nu_1}{2k-1},\ \gamma^{-(2)}_{n,k}=\frac{2n+3}{2k+3},$$

$$\lambda^{+(1)}_{n,k}=\frac{k+1-2nk-3n}{(k+1)(2k+3)},\ \lambda^{-(1)}_{n,k}=\frac{2nk+3k-n-1}{(n+1)(2k-1)}.$$

As is known, the general solution of the inhomogeneous equation (1) in the domain Ω_j ($j=1\div2$) can be written in the following form:

$$\vec{U}_j(\vec{x})=\vec{U}^G_j(\vec{x})+\vec{U}^T_j(\vec{x}), \tag{31}$$

where $\vec{U}^G_j(\vec{x})$ is a general solution of the corresponding homogeneous equation, $\vec{U}^T_j(\vec{x})$ is a partial solution of a non-homogeneous equation (thermal displacements). Due to the basis nature of solutions (19), (20), the general solution of the homogeneous equation (1) in the domains $\{\Omega_j\}_{j=1}^2$ can be written as follows:

$$\vec{U}^G_1(\vec{x})=\sum_{n=1}^{\infty}a^{(1)}_{1,n}R_1^{-n+2}\vec{W}^{-}_{1,n}(r_1,\theta_1)+\sum_{n=0}^{\infty}a^{(1)}_{2,n}R_1^{-n}\vec{W}^{-}_{2,n}(r_1,\theta_1)+\sum_{n=0}^{\infty}a^{(2)}_{1,n}R_2^{n+3}\vec{W}^{+}_{1,n}(r_2,\theta_2)+\sum_{n=1}^{\infty}a^{(2)}_{2,n}R_2^{n+1}\vec{W}^{+}_{2,n}(r_2,\theta_2),\ \vec{x}\in\Omega_1; \tag{32}$$

$$\vec{U}^G_2(\vec{x})=\sum_{n=1}^{\infty}b_{1,n}R_2^{-n+2}\vec{W}^{-}_{1,n}(r_2,\theta_2)+\sum_{n=0}^{\infty}b_{2,n}R_2^{-n}\vec{W}^{-}_{2,n}(r_2,\theta_2),\ \vec{x}\in\Omega_2. \tag{33}$$

Here $a^{(j)}_{i,n}$, $b_{i,n}$ are the unknown parameters of the model.

We will look for a partial solution $\vec{U}^T_j(\vec{x})$ in the domain Ω_j in the form

$$\vec{U}^T_j(\vec{x})=\vec{\nabla}\Phi_j(\vec{x}).$$

Then we obtain the Poisson equation for the function $\Phi_j(\vec{x})$

$$\Delta\Phi_j(\vec{x})=2\tilde{\alpha}_jT_j(\vec{x}),\ \vec{x}\in\Omega_j,\ \tilde{\alpha}_j=\frac{\alpha_j}{2}\frac{1+\nu_j}{1-\nu_j},$$

whose solution can be written as:

$$\Phi_1(\vec{x})=\tilde{\alpha}_1\sum_{n=0}^{\infty}\frac{R_1^{-n}t_n^{(1)}}{2n+3}r_1^2w_n^-(r_1,\theta_1)-\tilde{\alpha}_1\sum_{n=0}^{\infty}\frac{R_2^{n+1}t_n^{(2)}}{2n-1}r_1^2w_n^+(r_2,\theta_2),$$

$$\Phi_2(\vec{x})=\tilde{\alpha}_2\sum_{n=0}^{\infty}\frac{R_2^{-n}}{2n+3}\left[r_2^2c_n-\frac{r_2^4g_n}{4(2n+5)}\right]w_n^-(r_2,\theta_2).$$

Thus, the vectors of thermal displacements in the domains $(\Omega_i)_{i=1}^2$ are given by the formulas

$$\vec{U}^T_1(\vec{x})=\tilde{\alpha}_1\sum_{n=0}^{\infty}\frac{R_1^{-n}t_n^{(1)}}{2n+3}\vec{V}^-_n(r_1,\theta_1)-\tilde{\alpha}_1\sum_{n=0}^{\infty}\frac{R_2^{n+1}t_n^{(2)}}{2n-1}\vec{V}^+_n(r_2,\theta_2),\ \vec{x}\in\Omega_1; \tag{34}$$

$$\vec{U}^T_2(\vec{x})=-\tilde{\alpha}_2\sum_{n=0}^{\infty}\frac{R_2^{-n}g_n}{4(2n+5)(2n+3)}\vec{V}^{-(1)}_n(r_2,\theta_2)+$$

ISSN 1814-4225 (print)
ISSN 2663-2012 (online)

$$+\tilde{\alpha}_2\sum_{n=0}^{\infty}\frac{R_2^{-n}c_n}{2n+3}\vec{V}_n^-(r_2,\theta_2),\ \ \vec{x}\in\Omega_2. \qquad (35)$$

Formulas (25) – (30) allow us to write a vector function $\vec{U}_1(\vec{x})$ in a spherical coordinate system with the origin at the point O_j

$$\vec{U}_1(r_1,\theta_1)=\sum_{n=0}^{\infty}\vec{W}_{1,n}^+(r_1,\theta_1)\sum_{k=0}^{n}C_n^k z_{12}^{n-k}R_2^{k+3}a_{1,k}^{(2)}+$$

$$+\sum_{n=1}^{\infty}a_{1,n}^{(1)}R_1^{-n+2}\vec{W}_{1,n}^-(r_1,\theta_1)+\sum_{n=0}^{\infty}a_{2,n}^{(1)}R_1^{-n}\vec{W}_{2,n}^-(r_1,\theta_1)+$$

$$+\sum_{n=1}^{\infty}\vec{W}_{2,n}^+(r_1,\theta_1)\sum_{k=1}^{n}C_{n-1}^{k-1}\gamma_{k,n}^{+(2)}z_{12}^{n-k}R_2^{k+1}a_{2,k}^{(2)}+$$

$$+\sum_{n=0}^{\infty}\vec{W}_{1,n}^+(r_1,\theta_1)\sum_{k=1}^{n+1}C_n^{k-1}\gamma_{k,n}^{+(1)}z_{12}^{n-k+2}R_2^{k+1}a_{2,k}^{(2)}+$$

$$+\tilde{\alpha}_1\sum_{n=0}^{\infty}\frac{t_n^{(1)}}{2n+3}R_1^{-n}\vec{V}_n^-(r_1,\theta_1)-$$

$$-\tilde{\alpha}_1\sum_{n=0}^{\infty}\vec{V}_n^+(r_1,\theta_1)\sum_{k=0}^{n}C_n^k\gamma_{k,n}^{+(2)}z_{12}^{n-k}\frac{R_2^{k+1}t_k^{(2)}}{2k-1}-$$

$$-\tilde{\alpha}_1\sum_{n=0}^{\infty}\vec{W}_{1,n}^+(r_1,\theta_1)\sum_{k=1}^{n+1}C_{n+1}^k\lambda_{k,n}^{+(1)}z_{12}^{n-k+2}\frac{R_2^{k+1}t_k^{(2)}}{2k-1},\quad (36)$$

$$\vec{U}_1(r_2,\theta_2)=\sum_{n=1}^{\infty}\vec{W}_{1,n}^-(r_2,\theta_2)\sum_{k=n}^{\infty}C_k^n z_{12}^{k-n}R_1^{-k+2}a_{1,k}^{(1)}+$$

$$+\sum_{n=0}^{\infty}a_{1,n}^{(2)}R_2^{n+3}\vec{W}_{1,n}^+(r_2,\theta_2)+\sum_{n=1}^{\infty}a_{2,n}^{(2)}R_2^{n+1}\vec{W}_{2,n}^+(r_2,\theta_2)+$$

$$+\sum_{n=0}^{\infty}\vec{W}_{2,n}^-(r_2,\theta_2)\sum_{k=n}^{\infty}C_{k+1}^{n+1}\gamma_{k,n}^{-(2)}z_{12}^{k-n}R_1^{-k}a_{2,k}^{(1)}+$$

$$+\sum_{n=1}^{\infty}\vec{W}_{1,n}^-(r_2,\theta_2)\sum_{k=n-1}^{\infty}C_{k+1}^n\gamma_{k,n}^{-(1)}z_{12}^{k-n+2}R_1^{-k}a_{2,k}^{(1)}-$$

$$-\tilde{\alpha}_1\sum_{n=0}^{\infty}\frac{t_n^{(2)}}{2n-1}R_2^{n+1}\vec{V}_n^+(r_2,\theta_2)+$$

$$+\tilde{\alpha}_1\sum_{n=0}^{\infty}\vec{V}_n^-(r_2,\theta_2)\sum_{k=n}^{\infty}C_k^n\gamma_{k,n}^{-(2)}z_{12}^{k-n}\frac{R_1^{-k}t_k^{(1)}}{2k+3}+$$

$$+\tilde{\alpha}_1\sum_{n=1}^{\infty}\vec{W}_{1,n}^-(r_2,\theta_2)\sum_{k=n-1}^{\infty}C_{k+1}^n\lambda_{k,n}^{-(1)}z_{12}^{k-n+2}\frac{R_1^{-k}t_k^{(1)}}{2k+3}.\quad (37)$$

According to formulas (31), (33)

$$\vec{U}_2(r_2,\theta_2)=\sum_{n=1}^{\infty}b_{1,n}R_2^{-n+2}\vec{W}_{1,n}^-(r_2,\theta_2)+$$

$$+\sum_{n=0}^{\infty}b_{2,n}R_2^{-n}\vec{W}_{2,n}^-(r_2,\theta_2)+\tilde{\alpha}_2\sum_{n=0}^{\infty}\frac{c_n}{2n+3}\vec{V}_n^-(r_2,\theta_2)-$$

$$-\tilde{\alpha}_2\sum_{n=0}^{\infty}\frac{R_2^{-n}g_n}{4(2n+3)(2n+5)}\vec{V}_n^{-(1)}(r_2,\theta_2).\quad (38)$$

Let us pass in formulas (36) – (38) to the coordinate form, and also in formulas (37), (38) from displacements to the corresponding stresses on the surface Γ_2 with the normal vector $\vec{n}_2=\vec{e}_{r_2}$. After satisfying the boundary condition (4) and the conjugation conditions (6), we obtain an infinite system of linear algebraic equations with respect to the unknown parameters

$$na_{1,n}^{(1)}+\beta_{1,n}^{-(1)}a_{2,n}^{(1)}-(n+1)\sum_{k=0}^{n}u_{n,k}^{+(1)}a_{1,k}^{(2)}+\beta_{1,n}^{+(1)}\sum_{k=1}^{n}u_{n,k}^{+(2)}a_{2,k}^{(2)}-$$

$$-(n+1)\sum_{k=1}^{n+1}u_{n,k}^{+(3)}a_{2,k}^{(2)}+\tilde{\alpha}_1\frac{(n+2)t_n^{(1)}}{2n+3}+$$

$$+\tilde{\alpha}_1(n-1)\sum_{k=0}^{n}u_{n,k}^{+(4)}\frac{t_k^{(2)}}{2k-1}+\tilde{\alpha}_1(n+1)\sum_{k=1}^{n+1}u_{n,k}^{+(5)}\frac{t_k^{(2)}}{2k-1}=0,\ (39)$$

$$a_{1,n}^{(1)}+\beta_{2,n}^{-(1)}a_{2,n}^{(1)}+\sum_{k=0}^{n}u_{n,k}^{+(1)}a_{1,k}^{(2)}+\beta_{2,n}^{+(1)}\sum_{k=1}^{n}u_{n,k}^{+(2)}a_{2,k}^{(2)}+$$

$$+\sum_{k=1}^{n+1}u_{n,k}^{+(3)}a_{2,k}^{(2)}+\tilde{\alpha}_1\frac{t_n^{(1)}}{2n+3}-$$

$$-\tilde{\alpha}_1\sum_{k=0}^{n}u_{n,k}^{+(4)}\frac{t_k^{(2)}}{2k-1}-\tilde{\alpha}_1\sum_{k=1}^{n+1}u_{n,k}^{+(5)}\frac{t_k^{(2)}}{2k-1}=0,\qquad (40)$$

$$-(n+1)a_{1,n}^{(2)}+\beta_{1,n}^{+(1)}a_{2,n}^{(2)}+n\sum_{k=n}^{\infty}u_{n,k}^{-(1)}a_{1,k}^{(1)}+$$

$$+\beta_{1,n}^{-(1)}\sum_{k=n}^{\infty}u_{n,k}^{-(2)}a_{2,k}^{(1)}+n\sum_{k=n-1}^{\infty}u_{n,k}^{-(3)}a_{2,k}^{(1)}+$$

$$+\tilde{\alpha}_1\frac{(n-1)t_n^{(2)}}{2n-1}+\tilde{\alpha}_1(n+2)\sum_{k=n}^{\infty}u_{n,k}^{-(4)}\frac{t_k^{(1)}}{2k+3}+$$

$$+\tilde{\alpha}_1 n\sum_{k=n-1}^{\infty}u_{n,k}^{-(5)}\frac{t_k^{(1)}}{2k+3}=nb_{1,n}+\beta_{1,n}^{-(2)}b_{2,n}-$$

$$-\tilde{\alpha}_2\frac{(n+4)g_nR_2^2}{4(2n+3)(2n+5)}+\tilde{\alpha}_2\frac{(n+2)c_n}{2n+3},\qquad (41)$$

$$a_{1,n}^{(2)}+\beta_{2,n}^{+(1)}a_{2,n}^{(2)}+\sum_{k=n}^{\infty}u_{n,k}^{-(1)}a_{1,k}^{(1)}+\beta_{2,n}^{-(1)}\sum_{k=n}^{\infty}u_{n,k}^{-(2)}a_{2,k}^{(1)}+$$

$$+\sum_{k=n-1}^{\infty}u_{n,k}^{-(3)}a_{2,k}^{(1)}-\tilde{\alpha}_1\frac{t_n^{(2)}}{2n-1}+\tilde{\alpha}_1\sum_{k=n}^{\infty}u_{n,k}^{-(4)}\frac{t_k^{(1)}}{2k+3}+$$

$$+\tilde{\alpha}_1\sum_{k=n-1}^{\infty}u_{n,k}^{-(5)}\frac{t_k^{(1)}}{2k+3}=b_{1,n}+\beta_{2,n}^{-(2)}b_{2,n}-$$

$$-\tilde{\alpha}_2\frac{g_nR_2^2}{4(2n+3)(2n+5)}+\tilde{\alpha}_2\frac{c_n}{2n+3}, \qquad (42)$$

$$(n+2)(n+1)a_{1,n}^{(2)}+\rho_{1,n}^{+(1)}a_{2,n}^{(2)}+n(n-1)\sum_{k=n}^{\infty}u_{n,k}^{-(1)}a_{1,k}^{(1)}+$$

$$+\rho_{1,n}^{-(1)}\sum_{k=n}^{\infty}u_{n,k}^{-(2)}a_{2,k}^{(1)}+n(n-1)\sum_{k=n-1}^{\infty}u_{n,k}^{-(3)}a_{2,k}^{(1)}-$$

$$-\tilde{\alpha}_1\frac{\left[n(n-1)+2(2n-1)\right]t_n^{(2)}}{2n-1}+$$

$$+\tilde{\alpha}_1\left[(n+1)(n+2)-2(2n+3)\right]\sum_{k=n}^{\infty}u_{n,k}^{-(4)}\frac{t_k^{(1)}}{2k+3}+$$

$$+\tilde{\alpha}_1 n(n-1)\sum_{k=n-1}^{\infty}u_{n,k}^{-(5)}\frac{t_k^{(1)}}{2k+3}=$$

$$=\frac{G_2}{G_1}\left\{n(n-1)b_{1,n}+\rho_{1,n}^{-(2)}b_{2,n}+\right.$$

$$-\tilde{\alpha}_2\frac{\left[(n+3)(n+4)-4(2n+5)\right]g_nR_2^2}{4(2n+3)(2n+5)}+$$

$$\left.+\tilde{\alpha}_2\frac{\left[(n+1)(n+2)-2(2n+3)\right]c_n}{2n+3}\right\}, \qquad (43)$$

$$-(n+2)a_{1,n}^{(2)}+\rho_{2,n}^{+(1)}a_{2,n}^{(2)}+(n-1)\sum_{k=n}^{\infty}u_{n,k}^{-(1)}a_{1,k}^{(1)}+$$

$$+\rho_{2,n}^{-(1)}\sum_{k=n}^{\infty}u_{n,k}^{-(2)}a_{2,k}^{(1)}+(n-1)\sum_{k=n-1}^{\infty}u_{n,k}^{-(3)}a_{2,k}^{(1)}-$$

$$+\tilde{\alpha}_1\frac{nt_n^{(2)}}{2n-1}+\tilde{\alpha}_1(n+1)\sum_{k=n}^{\infty}u_{n,k}^{-(4)}\frac{t_k^{(1)}}{2k+3}+$$

$$+\tilde{\alpha}_1(n-1)\sum_{k=n-1}^{\infty}u_{n,k}^{-(5)}\frac{t_k^{(1)}}{2k+3}=$$

$$=\frac{G_2}{G_1}\left\{(n-1)b_{1,n}+\rho_{2,n}^{-(2)}b_{2,n}+\right.$$

$$\left.-\tilde{\alpha}_2\frac{(n+3)g_nR_2^2}{4(2n+3)(2n+5)}+\tilde{\alpha}_2\frac{(n+1)c_n}{2n+3}\right\}, \qquad (44)$$

where

$$\beta_{1,n}^{+(j)}=-n(n+3-4\nu_j),\ \beta_{2,n}^{+(j)}=n+4\nu_j-4,$$

$$\beta_{1,n}^{-(j)}=(n+1)(n+4\nu_j-2),\ \beta_{2,n}^{-(j)}=n-4\nu_j+5,$$

$$\rho_{1,n}^{+(j)}=n(n^2+3n-2\nu_j),\ \rho_{2,n}^{+(j)}=-(n^2+2\nu_j-2),$$

$$\rho_{1,n}^{-(j)}=(n+1)(n^2-n-2\nu_j-2),\ \rho_{2,n}^{-(j)}=n^2+2n+2\nu_j-1,$$

$$u_{n,k}^{+(1)}=C_n^k\omega_{n+3,k+3},\ u_{n,k}^{-(1)}=C_k^n\omega_{k-2,n-2},$$

$$u_{n,k}^{+(2)}=C_{n-1}^{k-1}\gamma_{k,n}^{+(2)}\omega_{n+1,k+1},\ u_{n,k}^{-(2)}=C_{k+1}^{n+1}\gamma_{k,n}^{-(2)}\omega_{k,n},$$

$$u_{n,k}^{+(3)}=C_n^{k-1}\gamma_{k,n}^{+(1)}\omega_{n+3,k+1},\ u_{n,k}^{-(3)}=C_{k+1}^{n}\gamma_{k,n}^{-(1)}\omega_{k,n-2},$$

$$u_{n,k}^{+(4)}=C_n^k\gamma_{k,n}^{+(2)}\omega_{n+1,k+1},\ u_{n,k}^{-(4)}=C_k^n\gamma_{k,n}^{-(2)}\omega_{k,n},$$

$$u_{n,k}^{+(5)}=C_{n+1}^{k}\lambda_{k,n}^{+(1)}\omega_{n+3,k+1},\ u_{n,k}^{-(5)}=C_{k+1}^{n}\lambda_{k,n}^{-(1)}\omega_{k,n-2}.$$

After eliminating unknowns $b_{i,n}$ and some transformations, the system (39) – (44) can be represented as

$$a_{1,n}^{(1)}+\frac{(n+1)(2n+3)}{2n+1}a_{2,n}^{(1)}-\frac{\Delta_n^{-(1)}+2}{2n+1}\sum_{k=1}^{n}u_{n,k}^{+(2)}a_{2,k}^{(2)}=$$

$$=-\tilde{\alpha}_1\frac{t_n^{(1)}}{2n+1}+\tilde{\alpha}_1\frac{2}{2n+1}\sum_{k=0}^{n}u_{n,k}^{+(4)}\frac{t_k^{(2)}}{2k-1}, \qquad (45)$$

$$n=1\div\infty;$$

$$a_{2,n}^{(1)}+\frac{2n+1}{\Delta_n^{-(1)}}\sum_{k=0}^{n}u_{n,k}^{+(1)}a_{1,k}^{(2)}+\frac{n(2n-1)}{\Delta_n^{-(1)}}\sum_{k=1}^{n}u_{n,k}^{+(2)}a_{2,k}^{(2)}+$$

$$+\frac{2n+1}{\Delta_n^{-(1)}}\sum_{k=1}^{n+1}u_{n,k}^{+(3)}a_{2,k}^{(2)}=\tilde{\alpha}_1\frac{2n-1}{\Delta_n^{-(1)}}\sum_{k=0}^{n}u_{n,k}^{+(4)}\frac{t_k^{(2)}}{2k-1}+$$

$$+\tilde{\alpha}_1\frac{2t_n^{(1)}}{(2n+3)\Delta_n^{-(1)}}+\tilde{\alpha}_1\frac{2n+1}{\Delta_n^{-(1)}}\sum_{k=1}^{n+1}u_{n,k}^{+(5)}\frac{t_k^{(2)}}{2k-1}, \qquad (46)$$

$$n=0\div\infty;$$

$$a_{2,n}^{(2)}+\frac{(1-G_{21})\xi_n}{\Delta_n^{(5)}}\sum_{k=n}^{\infty}u_{n,k}^{-(1)}a_{1,k}^{(1)}+\frac{(1-G_{21})\eta_n}{\Delta_n^{(5)}}\sum_{k=n}^{\infty}u_{n,k}^{-(2)}a_{2,k}^{(1)}+$$

$$+\frac{(1-G_{21})\xi_n}{\Delta_n^{(5)}}\sum_{k=n-1}^{\infty}u_{n,k}^{-(3)}a_{2,k}^{(1)}=\tilde{\alpha}_1\frac{(G_{21}-1)\eta_n}{(n+1)\Delta_n^{(5)}}\sum_{k=n}^{\infty}\frac{u_{n,k}^{-(4)}t_k^{(1)}}{2k+3}+$$

$$+\tilde{\alpha}_1\frac{(1-G_{21})\xi_n}{(2n+1)\Delta_n^{(5)}}\frac{2t_n^{(2)}}{2n-1}-\tilde{\alpha}_1\frac{(1-G_{21})\xi_n}{\Delta_n^{(5)}}\sum_{k=n-1}^{\infty}\frac{u_{n,k}^{-(5)}t_k^{(1)}}{2k+3}, \qquad (47)$$

$$n=1\div\infty;$$

$$a_{1,n}^{(2)}+\frac{n(2n-1)}{2n+1}a_{2,n}^{(2)}-\frac{\Delta_n^{(4)}}{(2n+1)\Delta_n^{(3)}}\sum_{k=n}^{\infty}u_{n,k}^{-(2)}a_{2,k}^{(1)}=$$

$$=\tilde{\alpha}_1\frac{t_n^{(2)}}{2n+1}+\tilde{\alpha}_1\frac{2}{2n+1}\sum_{k=n}^{\infty}u_{n,k}^{-(4)}\frac{t_k^{(1)}}{2k+3}+$$

$$+\tilde{\alpha}_2G_{21}\frac{(2-2\nu_2)g_nR_2^2}{(2n+5)\Delta_n^{-(2)}\Delta_n^{(3)}}-\tilde{\alpha}_2G_{21}\frac{(4-4\nu_2)c_n}{\Delta_n^{-(2)}\Delta_n^{(3)}}, \qquad (48)$$

$$n=0\div\infty;$$

$$b_{1,n}=\left[1-\frac{(2n+1)}{\Delta_n^{-(2)}}\beta_{2,n}^{-(2)}\right]a_{1,n}^{(2)}+\left[\beta_{2,n}^{+(1)}-\frac{n(2n-1)}{\Delta_n^{-(2)}}\beta_{2,n}^{-(2)}\right]a_{2,n}^{(2)}+$$

$$+\sum_{k=n}^{\infty}u_{n,k}^{-(1)}a_{1,k}^{(1)}+\left[\beta_{2,n}^{-(1)}-\frac{\Delta_n^{-(1)}}{\Delta_n^{-(2)}}\beta_{2,n}^{-(2)}\right]\sum_{k=n}^{\infty}u_{n,k}^{-(2)}a_{2,k}^{(1)}+$$

$$+\sum_{k=n-1}^{\infty}u_{n,k}^{-(3)}a_{2,k}^{(1)}-\tilde{\alpha}_1\left[\frac{1}{2n-1}-\frac{\beta_{2,n}^{-(2)}}{\Delta_n^{-(2)}}\right]t_n^{(2)}+$$

$$+\tilde{\alpha}_1\left[1+\frac{2\beta_{2,n}^{-(2)}}{\Delta_n^{-(2)}}\right]\sum_{k=n}^{\infty}u_{n,k}^{-(4)}\frac{t_k^{(1)}}{2k+3}+\tilde{\alpha}_1\sum_{k=n-1}^{\infty}u_{n,k}^{-(5)}\frac{t_k^{(1)}}{2k+3}+$$

$$+\tilde{\alpha}_2\frac{R_2^2g_n}{4(2n+3)(2n+5)}\left[1+4\frac{\beta_{2,n}^{-(2)}}{\Delta_n^{-(2)}}\right]-$$

ISSN 1814-4225 (print)
ISSN 2663-2012 (online)

$$-\tilde{\alpha}_2 \frac{c_n}{2n+3}\left[1+2\frac{\beta_{2,n}^{-(2)}}{\Delta_n^{-(2)}}\right], \quad (49)$$

$$n = 1 \div \infty;$$

$$b_{2,n} = \frac{2n+1}{\Delta_n^{-(2)}} a_{1,n}^{(2)} + \frac{n(2n-1)}{\Delta_n^{-(2)}} a_{2,n}^{(2)} + \frac{\Delta_n^{-(1)}}{\Delta_n^{-(2)}} \sum_{k=n}^{\infty} u_{n,k}^{-(2)} a_{2,k}^{(1)} -$$

$$-\tilde{\alpha}_1 \frac{1}{\Delta_n^{-(2)}} t_n^{(2)} - \tilde{\alpha}_1 \frac{2}{\Delta_n^{-(2)}} \sum_{k=n}^{\infty} u_{n,k}^{-(4)} \frac{t_k^{(1)}}{2k+3} -$$

$$-\tilde{\alpha}_2 \frac{R_2^2 g_n}{(2n+3)(2n+5)\Delta_n^{-(2)}} + \tilde{\alpha}_2 \frac{2c_n}{(2n+3)\Delta_n^{-(2)}}, \quad (50)$$

$$n = 0 \div \infty,$$

where

$$\Delta_n^{-(j)} = 2[(3-4\nu_j)n + 1 - 2\nu_j], \ j = 1,2;$$

$$d_n^{\pm(j)} = 2[n^2 + (1 \pm 2\nu_j)n + 1 \pm \nu_j], \ j = 1,2;$$

$$\Delta_n^{(3)} = n + 2 + G_{21}\frac{d_n^{+(2)}}{\Delta_n^{-(2)}}, \ \Delta_n^{(4)} = d_n^{+(1)} - G_{21} d_n^{+(2)} \frac{\Delta_n^{-(1)}}{\Delta_n^{-(2)}};$$

$$\Delta_n^{(5)} = d_n^{-(1)} + G_{21}(n-1)(\Delta_n^{-(1)} + 2), \ G_{21} = \frac{G_2}{G_1};$$

$$\xi_n = (n-1)(2n+1), \ \eta_n = (n-1)(n+1)(2n+3).$$

The following theorem formulates the conditions for the correct solution of system (45) – (48).

Theorem 3. The operator of the system (45) – (48) is a Fredholm operator in the space l_2^4 under the condition $z_{12} + R_2 < R_1$.

The proof of the theorem follows directly from the condition of the theorem, under which the series

$$\sum_{n=0}^{\infty} n^p \sum_{k=0}^{n} k^q C_n^k \omega_{n,k}$$

converges for arbitrary non-negative p, q.

5. Model for concentric inclusion

Let us consider the case of a concentric spherical inclusion, i.e., when $z_{12} = 0$. The corresponding parametric models can be obtained from formulas (8), (9), (31) – (35) by passing to the limit as $z_{12} \to 0$

$$T_1(\vec{x}) = \sum_{n=0}^{\infty} t_n^{(1)} R_1^{-n} w_n^-(r_1, \theta_1) +$$

$$+\sum_{n=0}^{\infty} t_n^{(2)} R_2^{n+1} w_n^+(r_1, \theta_1), \ \vec{x} \in \Omega_1; \quad (51)$$

$$T_2(\vec{x}) = \sum_{n=0}^{\infty}\left[2c_n - \frac{g_n r_1^2}{2n+3}\right]\frac{w_n^-(r_1, \theta_1)}{2R_2^n}, \ \vec{x} \in \Omega_2; \quad (52)$$

$$\vec{U}_1(\vec{x}) = \sum_{n=1}^{\infty} a_{1,n}^{(1)} R_1^{-n+2} \vec{W}_{1,n}^-(r_1, \theta_1) +$$

$$+\sum_{n=0}^{\infty} a_{2,n}^{(1)} R_1^{-n} \vec{W}_{2,n}^-(r_1, \theta_1) + \sum_{n=0}^{\infty} a_{1,n}^{(2)} R_2^{n+3} \vec{W}_{1,n}^+(r_1, \theta_1) +$$

$$+\sum_{n=1}^{\infty} a_{2,n}^{(2)} R_2^{n+1} \vec{W}_{2,n}^+(r_1, \theta_1) + \tilde{\alpha}_1 \sum_{n=0}^{\infty} \frac{R_1^{-n} t_n^{(1)}}{2n+3} \vec{V}_n^-(r_1, \theta_1) -$$

$$-\tilde{\alpha}_1 \sum_{n=0}^{\infty} \frac{R_2^{n+1} t_n^{(2)}}{2n-1} \vec{V}_n^+(r_1, \theta_1), \ \vec{x} \in \Omega_1; \quad (53)$$

$$\vec{U}_2(\vec{x}) = \sum_{n=1}^{\infty} b_{1,n} R_2^{-n+2} \vec{W}_{1,n}^-(r_1, \theta_1) +$$

$$+\sum_{n=0}^{\infty} b_{2,n} R_2^{-n} \vec{W}_{2,n}^-(r_1, \theta_1) + \tilde{\alpha}_2 \sum_{n=0}^{\infty} \frac{R_2^{-n} c_n}{2n+3} \vec{V}_n^-(r_1, \theta_1) -$$

$$-\tilde{\alpha}_2 \sum_{n=0}^{\infty} \frac{R_2^{-n} g_n}{4(2n+3)(2n+5)} \vec{V}_n^{-(1)}(r_1, \theta_1), \ \vec{x} \in \Omega_2. \quad (54)$$

Then for the parameters of the models we obtain systems of equations that follow from systems (16) – (18), (45) – (50)

$$t_n^{(1)} + \rho^{n+1} t_n^{(2)} = T_0 \delta_{n,0}, \ n = 0 \div \infty; \quad (55)$$

$$t_n^{(2)} + \frac{(k_2 - k_1)n}{k_2 n + k_1(n+1)} \rho^n t_n^{(1)} =$$

$$= \frac{k_2 R_2^2 g_n}{(2n+3)[k_2 n + k_1(n+1)]}, \ n = 0 \div \infty; \quad (56)$$

$$c_n = t_n^{(2)} + \rho^n t_n^{(1)} + \frac{R_2^2 g_n}{2(2n+3)}, \ n = 0 \div \infty; \quad (57)$$

$$(2n+1)a_{1,n}^{(1)} + (n+1)(2n+3)a_{2,n}^{(1)} - (\Delta_n^{-(1)} + 2)\rho^{n+1} a_{2,n}^{(2)} =$$

$$= -\tilde{\alpha}_1 t_n^{(1)} + \tilde{\alpha}_1 \frac{2\rho^{n+1}}{2n-1} t_n^{(2)}, \ n = 1 \div \infty; \quad (58)$$

$$\Delta_n^{-(1)} a_{2,n}^{(1)} + (2n+1)\rho^{n+3} a_{1,n}^{(2)} + n(2n-1)\rho^{n+1} a_{2,n}^{(2)} =$$

$$= \tilde{\alpha}_1 \frac{2t_n^{(1)}}{(2n+3)} + \tilde{\alpha}_1 \rho^{n+1} t_n^{(2)}, \ n = 0 \div \infty; \quad (59)$$

$$\Delta_n^{(5)} a_{2,n}^{(2)} + (1 - G_{21})\xi_n \rho^{n-2} a_{1,n}^{(1)} + (1 - G_{21})\eta_n \rho^n a_{2,n}^{(1)} =$$

$$= \tilde{\alpha}_1 (1 - G_{21}) \frac{2(n-1)}{(2n-1)} t_n^{(2)} - \tilde{\alpha}_1 (1 - G_{21})(n-1)\rho^n t_n^{(1)}, \quad (60)$$

$$n = 1 \div \infty;$$

$$(2n+1)\Delta_n^{(3)} a_{1,n}^{(2)} + n(2n-1)\Delta_n^{(3)} a_{2,n}^{(2)} - \Delta_n^{(4)} \rho^n a_{2,n}^{(1)} =$$

$$= \tilde{\alpha}_1 \Delta_n^{(3)} t_n^{(2)} + \tilde{\alpha}_1 \frac{2\Delta_n^{(3)} \rho^n}{2n+3} t_n^{(1)} - \tilde{\alpha}_2 G_{21} \frac{(4-4\nu_2)(2n+1)c_n}{\Delta_n^{-(2)}} +$$

$$+\tilde{\alpha}_2 G_{21} \frac{(2-2\nu_2)(2n+1) g_n R_2^2}{(2n+5)\Delta_n^{-(2)}}, \ n = 0 \div \infty; \quad (61)$$

$$b_{1,n} = \left[1 - \frac{(2n+1)}{\Delta_n^{-(2)}} \beta_{2,n}^{-(2)}\right] a_{1,n}^{(2)} + \left[\beta_{2,n}^{+(1)} - \frac{n(2n-1)}{\Delta_n^{-(2)}} \beta_{2,n}^{-(2)}\right] a_{2,n}^{(2)} +$$

$$+\rho^{n-2}a_{1,n}^{(1)}+\left[\beta_{2,n}^{-(1)}-\frac{\Delta_n^{-(1)}}{\Delta_n^{-(2)}}\beta_{2,n}^{-(2)}\right]\rho^n a_{2,n}^{(1)}-$$

$$-\tilde{\alpha}_1\left[\frac{1}{2n-1}-\frac{\beta_{2,n}^{-(2)}}{\Delta_n^{-(2)}}\right]t_n^{(2)}+\tilde{\alpha}_1\left[1+\frac{2\beta_{2,n}^{-(2)}}{\Delta_n^{-(2)}}\right]\frac{\rho^n t_n^{(1)}}{2n+3}+$$

$$+\tilde{\alpha}_2\frac{R_2^2 g_n}{4(2n+3)(2n+5)}\left[1+4\frac{\beta_{2,n}^{-(2)}}{\Delta_n^{-(2)}}\right]-$$

$$-\tilde{\alpha}_2\frac{c_n}{2n+3}\left[1+2\frac{\beta_{2,n}^{-(2)}}{\Delta_n^{-(2)}}\right],\ n=1\div\infty; \qquad (62)$$

$$b_{2,n}=\frac{2n+1}{\Delta_n^{-(2)}}a_{1,n}^{(2)}+\frac{n(2n-1)}{\Delta_n^{-(2)}}a_{2,n}^{(2)}+\frac{\Delta_n^{-(1)}}{\Delta_n^{-(2)}}\rho^n a_{2,n}^{(1)}-$$

$$-\tilde{\alpha}_1\frac{t_n^{(2)}}{\Delta_n^{-(2)}}-\tilde{\alpha}_1\frac{2\rho^n t_n^{(1)}}{(2n+3)\Delta_n^{-(2)}}+\tilde{\alpha}_2\frac{2c_n}{(2n+3)\Delta_n^{-(2)}}-$$

$$-\tilde{\alpha}_2\frac{R_2^2 g_n}{(2n+3)(2n+5)\Delta_n^{-(2)}},\ n=0\div\infty, \qquad (63)$$

where $\rho=R_2/R_1$.

As a result, the temperature field parameters $\{t_n^{(j)}\}_{n=0,j=1}^{\infty,2}$, $\{c_n\}_{n=0}^{\infty}$ are found directly

$$t_n^{(1)}=-\frac{k_2R_2^2g_n\rho^{n+1}}{(2n+3)[k_2n(1-\rho^{2n+1})+k_1(n+1+n\rho^{2n+1})]}+$$

$$+T_0\delta_{n,0}, \qquad (64)$$

$$t_n^{(2)}=\frac{k_2R_2^2g_n}{(2n+3)[k_2n(1-\rho^{2n+1})+k_1(n+1+n\rho^{2n+1})]}, \qquad (65)$$

$$c_n=\frac{k_2R_2^2g_n(1-\rho^{2n+1})}{(2n+3)[k_2n(1-\rho^{2n+1})+k_1(n+1+n\rho^{2n+1})]}+$$

$$+\frac{R_2^2g_n}{2(2n+3)}+T_0\delta_{n,0}. \qquad (66)$$

Before solving the system (58) – (61), let us analyze its determinant

$$\Delta_n(G_{21},\nu_1,\nu_2,\rho)=(2n+1)\cdot$$

$$\cdot\begin{vmatrix} 2n+1 & \psi_n^{(1)} & 0 & -\Delta_n^{(6)}\rho^{n+1} \\ 0 & \Delta_n^{-(1)} & \rho^{n+3} & \psi_n^{(2)}\rho^{n+1} \\ \tilde{G}\xi_n\rho^{n-2} & \tilde{G}\eta_n\rho^n & 0 & \Delta_n^{(5)} \\ 0 & -\Delta_n^{(4)}\rho^n & \Delta_n^{(3)} & \psi_n^{(2)}\Delta_n^{(3)} \end{vmatrix},$$

where

$$\psi_n^{(1)}=(n+1)(2n+3),\ \psi_n^{(2)}=n(2n-1),$$

$$\tilde{G}=1-G_{21},\ \Delta_n^{(6)}=\Delta_n^{-(1)}+2.$$

The following are the conditions for uniquely finding the parameters of the model (51) - (54).

Theorem 4. The determinant $\Delta_n(G_{21},\rho,\nu_1,\nu_2)$ of system (58) – (61) for $n\ge 1$, $\nu_j\in[-1,0.5)$, $R_{21}\in[0,1]$ does not vanish, moreover, the estimate is satisfied

$$|\Delta_n|\ge 2n(n+2)(2n+1)^2(2n^2+1). \qquad (67)$$

To prove the theorem, we will need the following new classical inequality

Lemma. For $\rho\in[0,1]$ and an arbitrary natural number n, the classical inequality holds

$$4(1-\rho^{2n-1}-\rho^{2n+3}+\rho^{4n+2})\ge$$

$$\ge(2n-1)(2n+3)(\rho^{2n-1}-2\rho^{2n+1}+\rho^{2n+3}). \qquad (68)$$

Proof of the lemma. We move all the terms (68) to one side and write the resulting expression as follows:

$$4(1-\rho^{2n-1}-\rho^{2n+3}+\rho^{4n+2})-$$

$$-(2n-1)(2n+3)(\rho^{2n-1}-2\rho^{2n+1}+\rho^{2n+3})=$$

$$=(1-\rho)^2\left[4\sum_{i=0}^{2n-2}\rho^i\sum_{k=0}^{2n+2}\rho^k-\right.$$

$$\left.-(2n-1)(2n+3)\rho^{2n-1}(1+\rho)^2\right].$$

Let us prove that the expression in square brackets is non-negative. Since $(1+\rho)^2\le 2(1+\rho^2)$, it is actually sufficient to prove the inequality

$$2\sum_{i=0}^{2n-2}\rho^i\sum_{k=0}^{2n+2}\rho^k-(2n-1)(2n+3)\rho^{2n-1}(1+\rho^2)\ge 0. \qquad (69)$$

By replacing the summation indices in the product of series, it can be represented as

$$\sum_{i=0}^{2n-2}\rho^i\sum_{k=0}^{2n+2}\rho^k=\sum_{m=0}^{2n-2}(m+1)\rho^m+(2n-1)\sum_{m=2n-1}^{2n+2}\rho^m+$$

$$+\sum_{m=2n+3}^{4n}(4n+1-m)\rho^m. \qquad (70)$$

Using identity (70), the left-hand side of inequality (69) can be transformed to the form

$$2\sum_{i=0}^{2n-2}\rho^i\sum_{k=0}^{2n+2}\rho^k-(2n-1)(2n+3)\rho^{2n-1}(1+\rho^2)=$$

$$=\sum_{m=1}^{2n-2}m(m+1)\left[\rho^{m-1}(1-\rho)-\rho^{4n-m}(1-\rho)\right]+$$

$$+2n(2n-1)\left[\rho^{2n-2}(1-\rho)-\rho^{2n+1}(1-\rho)\right]-$$

$$-(2n-1)\left[\rho^{2n-1}(1-\rho)-\rho^{2n}(1-\rho)\right]. \qquad (71)$$

All expressions in square brackets in (71) are non-negative at $\rho\in[0,1]$. In addition,

$$\left[\rho^{2n-2}(1-\rho)-\rho^{2n+1}(1-\rho)\right]\ge$$

$$\ge\left[\rho^{2n-1}(1-\rho)-\rho^{2n}(1-\rho)\right].$$

Consequently, inequality (69) is satisfied, and along with it the lemma is satisfied.

ISSN 1814-4225 (print)
ISSN 2663-2012 (online)

Proof of the theorem 4. The determinant of the system (58) – (61) after expansion can be represented as

$$\Delta_n(G_{21},\rho,\nu_1,\nu_2)=(2n+1)(I_0+I_1G_{21}+I_2G_{21}^2),$$

where

$$I_0=-(2n+1)(n+2)\Delta_n^{-(1)}d_n^{-(1)}-$$
$$-(n+2)\Delta_n^{-(1)}(\Delta_n^{-(1)}+2)\xi_n\rho^{2n-1}-$$
$$-(2n+1)d_n^{+(1)}d_n^{-(1)}\rho^{2n+3}-d_n^{+(1)}(\Delta_n^{-(1)}+2)\xi_n\rho^{4n+2}-$$
$$-\upsilon_n\rho^{2n-1}(1-\rho^2)^2,$$

$$I_1=-\frac{d_n^{+(2)}}{\Delta_n^{-(2)}}\vartheta_n\rho^{2n-1}(1-\rho^2)^2+\upsilon_n\rho^{2n-1}(1-\rho^2)^2-$$
$$-(\Delta_n^{-(1)}+2)d_n^{+(2)}\frac{\Delta_n^{-(1)}}{\Delta_n^{-(2)}}\xi_n(\rho^{2n-1}-\rho^{4n+2})-$$
$$-(2n+1)d_n^{+(2)}d_n^{-(1)}\frac{\Delta_n^{-(1)}}{\Delta_n^{-(2)}}\xi_n(1-\rho^{2n+3})-$$
$$-(\Delta_n^{-(1)}+2)d_n^{+(1)}\xi_n(\rho^{2n+3}-\rho^{4n+2})-$$
$$-(n+2)\Delta_n^{-(1)}(\Delta_n^{-(1)}+2)\xi_n(1-\rho^{2n-1}),$$

$$I_2=\vartheta_n\frac{d_n^{+(2)}}{\Delta_n^{-(2)}}\rho^{2n-1}(1-\rho^2)^2-$$
$$-\Delta_n^{-(1)}(\Delta_n^{-(1)}+2)\frac{d_n^{+(2)}}{\Delta_n^{-(2)}}\xi_n(1-\rho^{2n-1}-\rho^{2n+3}+\rho^{4n+2}),$$

where

$$\upsilon_n=(n-1)n(n+1)(n+2)(2n-1)(2n+1)(2n+3),$$
$$\vartheta_n=(n-1)n(n+1)(2n-1)(2n+1)(2n+3).$$

It is not difficult to understand that under the conditions of the theorem, expression I_0 is negative. In expression I_1 let's consider a combination of terms

$$\upsilon_n\rho^{2n-1}(1-\rho^2)^2-(n+2)\Delta_n^{-(1)}(\Delta_n^{-(1)}+2)\xi_n(1-\rho^{2n-1})$$

and evaluate its sign. Note that all other terms of I_1 are non-positive. Considering that

$$\min_{\nu_1\in[-1,\,0.5]}\Delta_n^{-(1)}(\Delta_n^{-(1)}+2)=4n(n+1), \tag{72}$$

the specified combination can be estimated from above by the expression

$$-n(n+1)(n+2)\xi_n\Big[4(1-\rho^{2n-1})-$$
$$-(2n-1)(2n+3)\rho^{2n-1}(1-\rho^2)^2\Big].$$

Using the lemma, we can conclude that the expression in square brackets is non-negative. Then the term highlighted above is not positive, and therefore $I_1\le 0$.

It remains to explore the sign I_2. Taking into account (72), I_2 can be estimated from above by the expression

$$I_2\le -n(n+1)\xi_n\frac{d_n^{+(2)}}{\Delta_n^{-(2)}}\Big[4(1-\rho^{2n-1}-\rho^{2n+3}+\rho^{4n+2})-$$
$$-(2n-1)(2n+3)\rho^{2n-1}(1-\rho^2)^2\Big]\le 0.$$

Here again the lemma is used.

Thus, it is proved that $I_0<0$, $I_1\le 0$, $I_2\le 0$ i.e. $\Delta_n<0$. Estimate (60) follows from the chain of inequalities

$$|\Delta_n|\ge(2n+1)|I_0|\ge(2n+1)^2(n+2)\Delta_n^{-(1)}d_n^{-(1)}$$

and the value of the minimum of the function

$$\min_{\nu_1\in[-1,\,0.5]}\Delta_n^{-(1)}d_n^{-(1)}=2n(2n^2+1).$$

Corollary to theorem 4. System (58) – (61) for $n\ge 1$ has a unique solution, which can be written as follows:

$$a_{1,n}^{(1)}=\tilde{\alpha}_1t_n^{(1)}\varepsilon_n^{(1)}\Big\{2[\Delta_n^{(5)}+\tilde{G}(n-1)\Delta_n^{(6)}\rho^{2n+1}]\Delta_n^{(3)}-$$
$$-\gamma_n^{(3)}\Delta_n^{(5)}\rho^{2n+3}-\tilde{G}(n-1)\gamma_n^{(3)}\Delta_n^{(6)}\rho^{4n+4}\Big\}+$$
$$+\tilde{\alpha}_1t_n^{(2)}\varepsilon_n^{(1)}\Big\{[d_n^{(5)}+2G_{21}\eta_n]\Delta_n^{(3)}\rho^{n+1}-$$
$$-\psi_n^{(1)}\Delta_n^{(3)}\gamma_n^{(4)}\rho^{n+3}+2\tilde{G}\eta_n\Delta_n^{(3)}\rho^{3n+2}-2\Delta_n^{(7)}\rho^{3n+4}\Big\}-$$
$$-\tilde{\alpha}_2G_{21}\frac{\varepsilon_n^{(2)}\tilde{g}_n}{\Delta_n^{-(2)}}\Big[\psi_n^{(1)}\Delta_n^{(5)}\rho^{n+3}+\tilde{G}\eta_n\Delta_n^{(6)}\rho^{3n+4}\Big], \tag{73}$$

$$a_{2,n}^{(1)}=\tilde{\alpha}_1t_n^{(1)}\frac{\varepsilon_n\Delta_n^{(3)}}{2n+3}\Big\{-2\Delta_n^{(5)}+\tilde{G}\xi_nd_n^{(4)}\rho^{2n-1}+$$
$$+(2n+1)[\tilde{G}n\xi_n+(4-4\nu_1)\gamma_n^{(4)}]\rho^{2n+3}-2\tilde{G}\psi_n^{(3)}\rho^{2n+1}+$$
$$+2\tilde{G}(n-1)\Delta_n^{(6)}\rho^{4n+2}\Big\}+\tilde{\alpha}_1t_n^{(2)}(2n+1)\varepsilon_n^{(1)}\Delta_n^{(3)}\cdot$$
$$\cdot\Big\{\gamma_n^{(4)}(\rho^{n+3}-\rho^{n+1})+2\tilde{G}(n-1)(\rho^{3n+2}-\rho^{3n})\Big\}+$$
$$+\tilde{\alpha}_2G_{21}\frac{(2n+1)\varepsilon_n^{(2)}}{\Delta_n^{-(2)}}\tilde{g}_n[\Delta_n^{(5)}\rho^{n+3}+$$
$$+\tilde{G}(n-1)\Delta_n^{(6)}\rho^{3n+2}], \tag{74}$$

$$a_{1,n}^{(2)}=\tilde{\alpha}_1t_n^{(1)}\varepsilon_n^{(1)}\Big\{2\tilde{G}\psi_n^{(4)}\Delta_n^{(3)}\rho^{n-2}-2\Delta_n^{(8)}\rho^{n}-$$
$$-\tilde{G}(n-1)\Delta_n^{(9)}\rho^{3n-1}+\tilde{G}\psi_n^{(4)}\gamma_n^{(3)}\rho^{3n+1}\Big\}+$$
$$+\tilde{\alpha}_1t_n^{(2)}\varepsilon_n^{(1)}\Big\{-[\gamma_n^{(4)}+2\tilde{G}(n-1)\rho^{2n-1}]\Delta_n^{-(1)}\Delta_n^{(3)}-$$
$$-\gamma_n^{(4)}\Delta_n^{(4)}\rho^{2n+1}-2\tilde{G}(n-1)\Delta_n^{(4)}\rho^{4n}\Big\}-$$
$$-\tilde{\alpha}_2G_{21}\frac{\varepsilon_n^{(2)}\tilde{g}_n}{\Delta_n^{-(2)}}\Big\{\Delta_n^{-(1)}\Delta_n^{(5)}+\tilde{G}\xi_n(2n+1)d_n^{(3)}\rho^{2n-1}-$$
$$-\tilde{G}\psi_n^{(2)}\eta_n\rho^{2n+1}\Big\}, \tag{75}$$

$$a_{2,n}^{(2)}=\tilde{\alpha}_1t_n^{(1)}\tilde{G}\varepsilon_n^{(1)}\xi_n\Big\{2\Delta_n^{(3)}(-\rho^{n-2}+\rho^{n})+$$
$$+\gamma_n^{(3)}(\rho^{3n+1}-\rho^{3n+3})\Big\}+$$
$$+\tilde{\alpha}_1t_n^{(2)}\tilde{G}\varepsilon_n\frac{(n-1)}{2n-1}\Big\{-2\Delta_n^{-(1)}\Delta_n^{(3)}+$$
$$+(2\Delta_n^{-(1)}-\psi_n^{(5)})\Delta_n^{(3)}\rho^{2n-1}+2\psi_n^{(5)}\Delta_n^{(3)}\rho^{2n+1}-$$

$$-[\psi_n^{(5)}\Delta_n^{(3)}+2\Delta_n^{(4)}]\rho^{2n+3}+2\Delta_n^{(4)}\rho^{4n+2}\Big\}+$$

$$+\tilde{\alpha}_2 G_{21}\tilde{G}\varepsilon_n^{(2)}\frac{\xi_n\psi_n^{(1)}}{\Delta_n^{-(2)}}\tilde{g}_n(\rho^{2n+1}-\rho^{2n+3}), \quad (76)$$

where

$$\varepsilon_n^{(j)}=\frac{(2-2\nu_j)(2n+1)^2}{\Delta_n},\ \varepsilon_n=\frac{(2n+1)^2}{\Delta_n},$$

$$\gamma_n^{(3)}=1+2G_{21}\frac{d_n^{+(2)}}{\Delta_n^{-(2)}},\ \gamma_n^{(4)}=1+2G_{21}(n-1),$$

$$d_n^{(3)}=n(n+1)+(4-4\nu_1)(2-4\nu_1),$$

$$d_n^{(4)}=n(2n+1)-8+8\nu_1,\ \psi_n^{(4)}=(n-1)n(2n-1),$$

$$d_n^{(5)}=2n^2-7n-1+8\nu_1(2n+1),$$

$$\psi_n^{(3)}=(n-1)n(2n-1)(2n+3),$$

$$\psi_n^{(5)}=(n+1)(2n-1)(2n+3),$$

$$\Delta_n^{(9)}=\psi_n^{(2)}\gamma_n^{(3)}+2\Delta_n^{(6)},\ \tilde{g}_n=\frac{g_n R_2^2}{(2n+5)}-2c_n,$$

$$\Delta_n^{(7)}=\tilde{G}\eta_n\Delta_n^{(3)}+\Delta_n^{(4)},\ \Delta_n^{(8)}=\tilde{G}\psi_n^{(4)}\Delta_n^{(3)}+\Delta_n^{(5)}.$$

The solution of system (58), (60) for $n=0$ has the following form:

$$a_{1,0}^{(2)}=-\tilde{\alpha}_1 t_0^{(1)}\frac{(4-4\nu_1)}{\tilde{\Delta}}-\tilde{\alpha}_1 t_0^{(2)}\frac{1}{\tilde{\Delta}}[\Delta_0^{-(1)}\Delta_0^{(3)}+\Delta_0^{(4)}\rho]-$$

$$-\tilde{\alpha}_2 G_{21}\frac{(2-2\nu_2)(1-2\nu_1)}{(1-2\nu_2)\tilde{\Delta}}\tilde{g}_0, \quad (77)$$

$$a_{2,0}^{(1)}=\frac{2}{3}\tilde{\alpha}_1 t_0^{(1)}\frac{\Delta_0^{(3)}}{\tilde{\Delta}}(\rho^3-1)+\tilde{\alpha}_1 t_0^{(2)}\frac{\Delta_0^{(3)}}{\tilde{\Delta}}(\rho^3-\rho)+$$

$$+\tilde{\alpha}_2 G_{21}\frac{(1-\nu_2)}{(1-2\nu_2)\tilde{\Delta}}\tilde{g}_0\rho^3, \quad (78)$$

where

$$\tilde{\Delta}=-2[2-4\nu_1+(1+\nu_1)\rho^3]-$$

$$-2G_{21}\frac{(1+\nu_2)(1-2\nu_1)}{1-2\nu_2}(1-\rho^3).$$

It is obvious that when the conditions of theorem 4 are met, $\Delta<0$.

Thus, in the case of a ball with a concentric spherical inclusion that releases heat according to the harmonic law, we have an exactly solvable models, defined by the formulas (51) – (54), (62) – (66), (73) – (78). Moreover, formulas (62) – (66), (73) – (76) for determining models parameters allow us to obtain the existence condition for the considered model.

The following theorem sets the conditions for the membership of model (51) – (54) to a certain class of functions.

Theorem 5. If the conditions of Theorem 4 are met and

$$\sum_{n=0}^{\infty}|g_n|<\infty,$$

the parametric models (51) – (54) exist and belong to the class functions

$$C^2(\Omega_1\cup\Omega_2)\cap C^1(\Omega_1\cup\overline{\Omega_2})\cap C(\overline{\Omega_1}\cup\overline{\Omega_2}).$$

The conclusion of the theorem follows directly from formulas (51) – (54), (62) – (66), (73) – (76), theorem 4 and the asymptotic estimates as $n\to\infty$

$$t_n^{(1)}=-\rho^{n+1}t_n^{(2)},\ t_n^{(2)}=O(n^{-2})|g_n|,\ c_n=O(n^{-1})|g_n|,$$

$$a_{1,n}^{(1)}=O(n^{-2}\rho^n)|g_n|,\ a_{2,n}^{(1)}=O(n^{-3}\rho^n)|g_n|,$$

$$a_{1,n}^{(2)}=O(n^{-3})|g_n|,\ a_{2,n}^{(2)}=O(n^{-4})|g_n|.$$

6. Model of the thermoelastic state of a loaded ball

Now we will construct the models of the temperature and thermoelastic fields in a loaded ball with a heat-active eccentric spherical inclusion subject to heat exchange between the ball and the environment. In the problem statement given in Section 2, we replace only conditions (3) and (4) with the following:

$$\left(\frac{\partial T_1}{\partial n}\right)_{\Gamma_1}=-\mu(T_1-T_0)_{\Gamma_1}, \quad (79)$$

$$(F\vec{U}_1)_{\Gamma_1}=-p\vec{e}_{r_1}. \quad (80)$$

Here, relation (79) specifies the condition of heat exchange between the ball and the environment, T_0 is the ambient temperature, μ is the heat exchange coefficient, p is the constant normal load acting on the surface of the ball. All other conditions of the problem statement in Section 2 remain unchanged.

We will construct parametric models of the temperature field and the field of thermoelastic displacements in the same form (8), (9), (31) – (35) as in sections 2, 3. The same method will be used. Obviously, only the resolving systems that link the model parameters will change. In the system (16) - (18) it is necessary to replace only equation (16) with the following:

$$t_n^{(1)}-\frac{n+1-\mu R_1}{n+\mu R_1}\sum_{k=0}^{n}C_n^k\omega_{n+1,k+1}t_k^{(2)}=$$

$$=T_0\delta_{n,0},\ n=0\div\infty. \quad (81)$$

In the system (45) – (48) it is necessary to replace equations (45), (46) with the following:

$$\xi_n a_{1,n}^{(1)}+\eta_n a_{2,n}^{(1)}+d_n^{-(1)}\sum_{k=1}^{n}u_{n,k}^{+(2)}a_{2,k}^{(2)}=$$

$$=-\frac{p}{2G_1}\delta_{n,0}-\tilde{\alpha}_1(n-1)t_n^{(1)}+2\tilde{\alpha}_1(n-1)\sum_{k=0}^{n}u_{n,k}^{+(4)}\frac{t_k^{(2)}}{2k-1}, \quad (82)$$

ISSN 1814-4225 (print)
ISSN 2663-2012 (online)

$$n=1\div\infty;$$

$$-d_n^{+(1)}a_{2,n}^{(1)}+n(n+2)(2n-1)\sum_{k=1}^{n}u_{n,k}^{+(2)}a_{2,k}^{(2)}+$$

$$+(2n+1)(n+2)\sum_{k=0}^{n}u_{n,k}^{+(1)}a_{1,k}^{(2)}+(2n+1)(n+2)\sum_{k=1}^{n+1}u_{n,k}^{+(3)}a_{2,k}^{(2)}=$$

$$=-\frac{p}{2G_1}\delta_{n,0}+\tilde{\alpha}_1(n+2)(2n-1)\sum_{k=0}^{n}u_{n,k}^{+(4)}\frac{t_k^{(2)}}{2k-1}+$$

$$+\tilde{\alpha}_1\frac{2(n+2)t_n^{(1)}}{2n+3}+\tilde{\alpha}_1(2n+1)(n+2)\sum_{k=1}^{n+1}u_{n,k}^{+(5)}\frac{t_k^{(2)}}{2k-1}, \quad (83)$$

$$n=0\div\infty.$$

Next, the conditions for the correct solution of the above systems are formulated.

Theorem 6. The operators of the systems (17), (81) and (47), (48), (82), (83) is Fredholm operators in the spaces l_2^2 and l_2^4 respectively under the condition $z_{12}+R_2<R_1$.

The proof is similar to the proof of theorem 3.

7. Loaded ball with concentric thermally active inclusion

Let us again consider separately the case of a concentric spherical cavity in a ball. Parametric models of the temperature field and the field of thermoelastic displacements are described by formulas (51) – (54). The equations for determining the parameters of the models are obtained from the system (55) – (62) by replacing the equations (55), (58), (59) with the following:

$$t_n^{(1)}-\frac{n+1-\mu R_1}{n+\mu R_1}\rho^{n+1}t_n^{(2)}=T_0\delta_{n,0}, \quad (84)$$

$$n=0\div\infty;$$

$$\xi_n a_{1,n}^{(1)}+\eta_n a_{2,n}^{(1)}+d_n^{-(1)}\rho^{n+1}a_{2,n}^{(2)}=$$

$$=-\frac{p}{2G_1}\delta_{n,0}-\tilde{\alpha}_1(n-1)t_n^{(1)}+\tilde{\alpha}_1\frac{2(n-1)}{2n-1}\rho^{n+1}t_n^{(2)}, \quad (85)$$

$$n=1\div\infty;$$

$$-d_n^{+(1)}a_{2,n}^{(1)}+(2n+1)(n+2)\rho^{n+3}a_{1,n}^{(2)}+$$

$$+n(n+2)(2n-1)\rho^{n+1}a_{2,n}^{(2)}=\tilde{\alpha}_1\frac{2(n+2)t_n^{(1)}}{2n+3}-$$

$$-\frac{p}{2G_1}\delta_{n,0}+\tilde{\alpha}_1(n+2)\rho^{n+1}t_n^{(2)},\ n=0\div\infty. \quad (86)$$

The parameters of the temperature field are found directly from the system of equations (56), (57), (84)

$$t_n^{(1)}=\frac{n+1-\mu R_1}{n+\mu R_1}\frac{k_2R_2^2g_n\rho^{n+1}}{(2n+3)[k_2n+k_1(n+1)]\tilde{d}_n}+$$

$$+T_0\delta_{n,o}, \quad (87)$$

$$t_n^{(2)}=\frac{k_2R_2^2g_n}{(2n+3)[k_2n+k_1(n+1)]\tilde{d}_n}, \quad (88)$$

$$c_n=\frac{k_2R_2^2g_n}{(2n+3)[k_2n+k_1(n+1)]\tilde{d}_n}\left[1+\frac{n+1-\mu R_1}{n+\mu R_1}\rho^{2n+1}\right]+$$

$$+\frac{R_2^2g_n}{2(2n+3)}+T_0\delta_{n,0}, \quad (89)$$

where

$$\tilde{d}_n=1+\frac{(k_2-k_1)n(n+1-\mu R_1)}{[k_2n+k_1(n+1)](n+\mu R_1)}\rho^{2n+1}.$$

The multiplier $\tilde{d}_n$, depending on the sign of the coefficient standing at ρ^{2n+1}, takes a minimum value either at $\rho=0$ or at $\rho=1$. Then

$$\tilde{d}_n\ge\min\left\{1,1+\frac{(k_2-k_1)n(n+1-\mu R_1)}{[k_2n+k_1(n+1)](n+\mu R_1)}\right\}.$$

Since

$$\min\left\{1+\frac{(k_2-k_1)n(n+1-\mu R_1)}{[k_2n+k_1(n+1)](n+\mu R_1)}\right\}\ge\min\left\{\frac{k_1}{k_2},\frac{k_2}{k_1}\right\},$$

then

$$\tilde{d}_n\ge\min\left\{\frac{k_1}{k_2},\frac{k_2}{k_1}\right\}. \quad (90)$$

Estimate (90) shows that the factor $\tilde{d}_n$ does not become zero for any admissible values of the parameters included in it.

To determine the parameters of the thermoelastic model from the system of equations (60), (61), (85), (86), it is first necessary to conduct an analysis of its determinant

$$\tilde{\Delta}_n(G_{21},\nu_1,\nu_2,\rho)=(2n+1)\xi_n\cdot$$

$$\cdot\begin{vmatrix}1 & \eta_n & 0 & d_n^{-(1)}\rho^{n+1}\\ 0 & -d_n^{+(1)} & (n+2)\rho^{n+3} & (n+2)\psi_n^{(2)}\rho^{n+1}\\ \tilde{G}\rho^{n-2} & \tilde{G}\eta_n\rho^n & 0 & \Delta_n^{(5)}\\ 0 & -\Delta_n^{(4)}\rho^n & \Delta_n^{(3)} & \psi_n^{(2)}\Delta_n^{(3)}\end{vmatrix}. \quad (91)$$

Similar to the justification of Theorem 4, the following statement can be proven [35].

Theorem 7. The determinant $\tilde{\Delta}_n(G_{21},\nu_1,\nu_2,\rho)$ of system (60), (61), (85), (86) for $n\ge2$, $\nu_j\in[-1,0.5)$, $\rho\in[0,1]$ does not vanish, moreover, the estimate is satisfied

$$|\tilde{\Delta}_n|\ge G_{21}^2(n^2-1)^3n(2n+1). \quad (92)$$

Corollary to theorem 7. System (60), (61), (85), (86) for $n\ge2$ has a unique solution, which can be written as follows:

$$a_{1,n}^{(1)}=-(n-1)\tilde{\varepsilon}_n^{(1)}\tilde{\alpha}_1t_n^{(1)}\left\{-\Delta_n^{(3)}\Delta_n^{(5)}+\tilde{G}d_n^{-(1)}\Delta_n^{(3)}\rho^{2n+1}+\right.$$

$$+(n+2)\gamma_n^{(3)}\Delta_n^{(5)}\rho^{2n+3}-\tilde{G}(n+2)\gamma_n^{(3)}d_n^{-(1)}\rho^{4n+4}\Big\}-$$
$$-\tilde{\varepsilon}_n^{(1)}\tilde{\alpha}_1 t_n^{(2)}\Big\{(n+2)\eta_n[\gamma_n^{(4)}\rho^{n+3}+\tilde{G}\rho^{3n+2}]\Delta_n^{(3)}-$$
$$-[(n+2)\eta_n\gamma_n^{(4)}+2G_{21}(n-1)d_n^{+(1)}]\Delta_n^{(3)}\rho^{n+1}+$$
$$+(n+2)[2G_{21}(n-1)\Delta_n^{(4)}-\tilde{G}\eta_n\Delta_n^{(3)}]\rho^{3n+4}\Big\}-$$
$$-\tilde{\alpha}_2 G_{21}\frac{\tilde{\varepsilon}_n^{(2)}(n+2)\eta_n}{\Delta_n^{-(2)}}\tilde{g}_n[\Delta_n^{(5)}\rho^{n+3}-\tilde{G}d_n^{-(1)}\rho^{3n+4}], \quad (93)$$

$$a_{2,n}^{(1)}=-\psi_n^{(8)}\tilde{\varepsilon}_n\Delta_n^{(3)}\tilde{\alpha}_1 t_n^{(1)}\{2\Delta_n^{(5)}+2\tilde{G}\psi_n^{(3)}\rho^{2n+1}-$$
$$-\tilde{G}[2d_n^{-(1)}+\psi_n^{(3)}]\rho^{2n-1}-[2\Delta_n^{(5)}+\tilde{G}\psi_n^{(3)}]\rho^{2n+3}+$$
$$+2\tilde{G}d_n^{-(1)}\rho^{4n+2}\}-(n+2)\tilde{\varepsilon}_n^{(1)}\xi_n\Delta_n^{(3)}\tilde{\alpha}_1 t_n^{(2)}\{\gamma_n^{(4)}\rho^{n+1}-$$
$$-\gamma_n^{(4)}\rho^{n+3}-\tilde{G}\rho^{3n}+\tilde{G}\rho^{3n+2}\}+\tilde{\alpha}_2 G_{21}\frac{\tilde{\varepsilon}_n^{(2)}(n+2)\xi_n}{\Delta_n^{-(2)}}\cdot$$
$$\cdot\tilde{g}_n(\Delta_n^{(5)}\rho^{n+3}-\tilde{G}d_n^{-(1)}\rho^{3n+2}), \quad (94)$$

$$a_{1,n}^{(2)}=(n-1)\tilde{\varepsilon}_n^{(1)}\tilde{\alpha}_1 t_n^{(1)}\Big\{\tilde{G}\psi_n^{(4)}\Delta_n^{(3)}\rho^{n-2}-\tilde{G}\psi_n^{(4)}\Delta_n^{(3)}\rho^{n}+$$
$$+(\gamma_n^{(3)}-1)\Delta_n^{(5)}\rho^{n}-\tilde{G}\psi_n^{(7)}\gamma_n^{(3)}\rho^{3n-1}-$$
$$-\tilde{G}(\gamma_n^{(3)}-1)d_n^{-(1)}\rho^{3n-1}+\tilde{G}\psi_n^{(7)}\gamma_n^{(3)}\rho^{3n+1}\Big\}+$$
$$+(n-1)\tilde{\varepsilon}_n^{(1)}\tilde{\alpha}_1 t_n^{(2)}\Big\{d_n^{+(1)}\Delta_n^{(3)}\gamma_n^{(4)}-\tilde{G}d_n^{+(1)}\Delta_n^{(3)}\rho^{2n-1}-$$
$$-(n+2)\gamma_n^{(4)}\Delta_n^{(4)}\rho^{2n+1}+\tilde{G}(n+2)\Delta_n^{(4)}\rho^{4n}\Big\}+$$
$$+\tilde{\alpha}_2 G_{21}\frac{\tilde{\varepsilon}_n^{(2)}(n-1)}{\Delta_n^{-(2)}}\tilde{g}_n\Big\{-d_n^{+(1)}\Delta_n^{(5)}-\tilde{G}\psi_n^{(1)}\psi_n^{(7)}\rho^{2n+1}+$$
$$+\tilde{G}[\psi_n^{(1)}\psi_n^{(7)}+d_n^{+(1)}d_n^{-(1)}]\rho^{2n-1}\Big\}, \quad (95)$$

$$a_{2,n}^{(2)}=\tilde{G}(n-1)\xi_n\tilde{\varepsilon}_n^{(1)}\tilde{\alpha}_1 t_n^{(1)}\Big\{-\Delta_n^{(3)}\rho^{n-2}+\Delta_n^{(3)}\rho^{n}+$$
$$+(n+2)\gamma_n^{(3)}\rho^{3n+1}-(n+2)\gamma_n^{(3)}\rho^{3n+3}\Big\}+$$
$$+\tilde{G}\frac{(n-1)}{2n-1}\tilde{\varepsilon}_n\tilde{\alpha}_1 t_n^{(2)}\Big\{2(n-1)d_n^{+(1)}\Delta_n^{(3)}-\xi_n d_n^{(6)}\Delta_n^{(3)}\rho^{2n-1}+$$
$$+2(n+2)(2n-1)\eta_n\Delta_n^{(3)}\rho^{2n+1}-(n+2)\xi_n\gamma_n^{(5)}\rho^{2n+3}+$$
$$+2(n-1)(n+2)\Delta_n^{(4)}\rho^{4n+2}\Big\}+$$
$$+\tilde{\alpha}_2 G_{21}\tilde{G}\frac{\tilde{\varepsilon}_n^{(2)}}{\Delta_n^{-(2)}}(n+2)\xi_n\eta_n\tilde{g}_n(\rho^{2n+1}-\rho^{2n+3}), \quad (96)$$

where

$$\psi_n^{(7)}=(n-1)n(n+2)(2n-1),\quad \psi_n^{(8)}=\frac{(n-1)(n+2)}{2n+3},$$
$$\tilde{\varepsilon}_n^{(j)}=\frac{(2-2\nu_j)(2n+1)^2}{\tilde{\Delta}_n},\quad \tilde{\varepsilon}_n=\frac{(2n+1)^2}{\tilde{\Delta}_n},$$
$$d_n^{(6)}=(n+1)(n+2)(2n+1)-4+4\nu_1.$$

System (61), (86) for n=0 has a solution

$$a_{2,0}^{(1)}=-\frac{p}{2G_1}\frac{\Delta_0^{(3)}}{\bar{\Delta}_0}+\frac{4}{3}\tilde{\alpha}_1 t_0^{(1)}\frac{\Delta_0^{(3)}}{\bar{\Delta}_0}(1-\rho^3)+$$
$$2\tilde{\alpha}_1 t_0^{(2)}\frac{\Delta_0^{(3)}}{\bar{\Delta}_0}\rho(1-\rho^2)-2\tilde{\alpha}_2 G_{21}\frac{2-2\nu_2}{\Delta_0^{-(2)}\bar{\Delta}_0}\tilde{g}_0\rho^3, \quad (97)$$

$$a_{1,0}^{(2)}=-\frac{p}{2G_1}\frac{\Delta_0^{(4)}}{\bar{\Delta}_0}+\frac{2}{3}\tilde{\alpha}_1 t_0^{(1)}\frac{2\Delta_0^{(4)}-d_0^{+(1)}\Delta_0^{(3)}}{\bar{\Delta}_0}+$$
$$+\tilde{\alpha}_1 t_0^{(2)}\frac{2\Delta_0^{(4)}\rho-d_0^{+(1)}\Delta_0^{(3)}}{\bar{\Delta}_0}-\tilde{\alpha}_2 G_{21}\frac{2-2\nu_2}{\Delta_0^{-(2)}\bar{\Delta}_0}\tilde{g}_0 d_0^{+(1)}, \quad (98)$$

where

$$\bar{\Delta}_0=-4(1+\nu_1)(1-\rho^3)-$$
$$-2G_{21}\frac{1+\nu_2}{1-2\nu_2}[1+\nu_1+2(1-2\nu_1)\rho^3].$$

From the last formula it follows that $\bar{\Delta}_0<0$.

It is necessary to consider separately the system (60), (61), (85), (86) for $n=1$, since in this case the determinant of the system is equal to zero. The condition of solvability of the system follows from the condition of statics on the outer boundary of the ball

$$\oiint_{\Gamma_1}(F\vec{U}_1(R_1,\theta_1),\vec{e}_z)dS=0$$

and coincides with two identical equations of the system

$$a_{2,1}^{(2)}=0. \quad (99)$$

The other two equations of the system have the form

$$-d_1^{+(1)}a_{2,1}^{(1)}+9\rho^4 a_{1,1}^{(2)}=3\tilde{\alpha}_1 t_1^{(2)}\rho^2+\frac{6}{5}\tilde{\alpha}_1 t_1^{(1)}, \quad (100)$$

$$3\Delta_1^{(3)}a_{1,1}^{(2)}-\Delta_1^{(4)}\rho a_{2,1}^{(1)}=\tilde{\alpha}_1\Delta_1^{(3)}t_1^{(2)}+\frac{2}{5}\tilde{\alpha}_1 t_1^{(1)}\Delta_1^{(3)}\rho+$$
$$+\tilde{\alpha}_2 G_{21}\frac{3(2-2\nu_2)}{\Delta_1^{-(2)}}\tilde{g}_1. \quad (101)$$

The determinant of the system (100), (101) is equal to

$$\bar{\Delta}_1=-54(1+\nu_1)(1-\rho^5)-$$
$$-27G_{21}\frac{1+\nu_2}{2-3\nu_2}[1+\nu_1+(4-6\nu_1)\rho^5],$$

from which it follows that for admissible values of the parameters it is negative. Then the solution of the system (100), (101) is given by the formulas

$$a_{2,1}^{(1)}=\frac{18}{5}\tilde{\alpha}_1 t_1^{(1)}\frac{\Delta_1^{(3)}(1-\rho^5)}{\bar{\Delta}_1}+9\tilde{\alpha}_1 t_1^{(2)}\frac{\Delta_1^{(3)}\rho^2(1-\rho^2)}{\bar{\Delta}_1}-$$
$$-27\tilde{\alpha}_2 G_{21}\frac{(2-2\nu_2)}{\Delta_1^{-(2)}\bar{\Delta}_1}\tilde{g}_1\rho^4, \quad (102)$$

$$a_{1,1}^{(2)}=\frac{2}{5}\tilde{\alpha}_1 t_1^{(1)}\frac{(3\Delta_1^{(4)}-d_1^{+(1)}\Delta_1^{(3)})\rho}{\bar{\Delta}_1}+$$
$$+\tilde{\alpha}_1 t_1^{(2)}\frac{-d_1^{+(1)}\Delta_1^{(3)}+3\Delta_1^{(4)}\rho^3}{\bar{\Delta}_1}-$$
$$-3\tilde{\alpha}_2 G_{21}\frac{(2-2\nu_2)}{\Delta_1^{-(2)}\bar{\Delta}_1}\tilde{g}_1 d_1^{+(1)}. \quad (103)$$

ISSN 1814-4225 (print)
ISSN 2663-2012 (online)

The parameter $a_{1,1}^{(1)}$ is chosen arbitrarily, which corresponds to the known fact that the solution of the second boundary value problem for a bounded body is determined uniquely up to the rigid displacement vector.

For the constructed model, as in Section 4, it is possible to guarantee that the temperature and stress fields belong to the class

$$C^2(\Omega_1 \bigcup \Omega_2) \bigcap C^1(\Omega_1 \bigcup \overline{\Omega_2}) \bigcap C(\overline{\Omega_1} \bigcup \overline{\Omega_2}).$$

8. Model of a loaded ball with a concentric inclusion having a heat-active spherical layer

Let us consider the model of the previous section in the case when heat is emitted not by the entire inclusion, but by its heat-active spherical layer.

We will use the above introduced notations taking into account the following change. We assume that the heat sources are located in the spherical layer of the inclusion, which occupies the domain $\Omega_2 = \{(r_1, \theta_1, \varphi_1) : R_3 < r_1 < R_2\}$ ($R_3 < R_2$), and in the rest of the inclusion $\Omega_3 = \{(r_1, \theta_1, \varphi_1) : 0 \le r_1 < R_3\}$ there are no heat sources. We will designate the internal boundary of the heat-active layer as Γ_3. The mathematical model of the thermoelastic state of the considered ball is a boundary value problem, which is described by a system of differential equations in partial derivatives (1), (2), where $j = 1 \div 3$, with boundary conditions (5), (6), (79), (80) and additional conditions on the boundary Γ_3

$$(T_2)_{|\Gamma_3} = (T_3)_{|\Gamma_3}, \left(\frac{\partial T_2}{\partial n_3}\right)_{|\Gamma_3} = \left(\frac{\partial T_3}{\partial n_3}\right)_{|\Gamma_3}; \quad (104)$$

$$(\vec{U}_2)_{|\Gamma_3} = (\vec{U}_3)_{|\Gamma_3}, \ (F\vec{U}_2)_{|\Gamma_3} = (F\vec{U}_3)_{|\Gamma_3}. \quad (105)$$

We will define the density of heat sources by the function $k_2 g(r_1)$, where

$$g(r_1) = R_2 g_0 (1 - R_3 / r_1) / (R_2 - R_3). \quad (106)$$

We construct the parametric model of the problem in a form similar to (51) - (54), but in view of (80), (106), we include in it functions that depend only on the radial variable

$$T_1(\vec{x}) = t_0^{(1)} w_0^-(r_1, \theta_1) + t_0^{(2)} R_2 w_0^+(r_1, \theta_1), \ \vec{x} \in \Omega_1; (107)$$

$$T_2(\vec{x}) = \left[c_0 - \frac{1}{6} g_0^- r_1^2\right] w_0^-(r_1, \theta_1) + \left[f_0 - \frac{1}{2} g_0^+ r_1^2\right] R_3 w_0^+(r_1, \theta_1), \ \vec{x} \in \Omega_2; \quad (108)$$

$$T_3(\vec{x}) = t_0^{(3)} w_0^-(r_1, \theta_1), \ \vec{x} \in \Omega_3; \quad (109)$$

$$\vec{U}_1(\vec{x}) = a_{2,0}^{(1)} \vec{W}_{2,0}^-(r_1, \theta_1) + a_{1,0}^{(2)} R_2^3 \vec{W}_{1,0}^+(r_1, \theta_1) + \frac{1}{3} \tilde{\alpha}_1 t_0^{(1)} \vec{V}_0^-(r_1, \theta_1) + \tilde{\alpha}_1 t_0^{(2)} R_2 \vec{V}_0^+(r_1, \theta_1), \ \vec{x} \in \Omega_1; (110)$$

$$\vec{U}_2(\vec{x}) = b_{1,0} R_3^3 \vec{W}_{1,0}^+(r_1, \theta_1) + b_{2,0} \vec{W}_{2,0}^-(r_1, \theta_1) + \frac{1}{3} \tilde{\alpha}_2 c_0 \vec{V}_0^-(r_1, \theta_1) - \frac{1}{60} \tilde{\alpha}_2 g_0^- \vec{V}_0^{-(1)}(r_1, \theta_1) - \frac{1}{12} \tilde{\alpha}_2 g_0^+ R_3 \vec{V}_0^{+(1)}(r_1, \theta_1) + \tilde{\alpha}_2 f_0 R_3 \vec{V}_0^+(r_1, \theta_1), \ \vec{x} \in \Omega_2; \quad (111)$$

$$\vec{U}_3(\vec{x}) = d_{2,0} \vec{W}_{2,0}^-(r_1, \theta_1) + \frac{1}{3} \tilde{\alpha}_2 t_0^{(3)} \vec{V}_0^-(r_1, \theta_1), \ \vec{x} \in \Omega_3, (112)$$

where $t_0^{(1)}, t_0^{(2)}, t_0^{(3)}, c_0, f_0, a_{2,0}^{(1)}, a_{1,0}^{(2)}, b_{1,0}, b_{2,0}, d_{2,0}$ are unknown parameters of the model which are in the process of modeling,

$$g_0^{\pm} = \pm R_2 g_0 / (R_2 - R_3).$$

After satisfying the boundary conditions and field conjugation conditions, the model parameters are found in the form

$$t_0^{(1)} = T_0 + \frac{(1 - \mu R_1)}{6 \mu R_1} k_{21} \tilde{g} (1 - \rho_2)^2 (2 + \rho_2) \rho_1, \ (113)$$

$$t_0^{(2)} = \frac{k_{21}}{6} \tilde{g} (1 - \rho_2)^2 (2 + \rho_2), \quad (114)$$

$$t_0^{(3)} = T_0 + \frac{\mu R_1 (1 - \rho_1) + \rho_1}{6 \mu R_1} k_{21} \tilde{g} (1 - \rho_2)^2 (2 + \rho_2) + \frac{\tilde{g}}{6} (1 - \rho_2)^3, \quad (115)$$

$$c_0 = T_0 + \frac{\mu R_1 (1 - \rho_1) + \rho_1}{6 \mu R_1} k_{21} \tilde{g} (1 - \rho_2)^2 (2 + \rho_2) + \frac{\tilde{g}}{6} (1 - 3\rho_2 - \rho_2^3), \quad (116)$$

$$f_0 = \frac{\tilde{g}}{6} \rho_2^2, \quad (117)$$

$$b_{1,0} = \frac{\tilde{\alpha}_2}{60} \tilde{g} \rho_2^2, \ b_{2,0} = d_{2,0}, \quad (118)$$

$$d_{2,0} = \frac{1}{q} \left\{ -\frac{p}{2G_1} + \frac{4}{3} \tilde{\alpha}_1 t_0^{(1)} (1 - \rho_1^3) + 2\tilde{\alpha}_1 t_0^{(2)} (\rho_1 - \rho_1^3) + -G_6 \left[\frac{2}{3} \tilde{\alpha}_2 T_0 + \frac{\tilde{\alpha}_2}{9} \frac{\mu R_1 (1 - \rho_1) + \rho_1}{\mu R_1} k_{21} \tilde{g} (1 - \rho_2)^2 (2 + \rho_2) - \frac{\tilde{\alpha}_2}{180} \tilde{g} (3\rho_2^5 - 10\rho_2^3 + 15\rho_2 - 8) \right] \right\}, \quad (119)$$

$$a_{2,0}^{(1)} = \frac{q_2}{q} \left[-\frac{p}{2G_1} + \frac{4}{3} \tilde{\alpha}_1 t_0^{(1)} (1 - \rho_1^3) + 2\tilde{\alpha}_1 t_0^{(2)} (\rho_1 - \rho_1^3) \right] + -G_4 \left[\frac{2}{3} \tilde{\alpha}_2 T_0 + \frac{\tilde{\alpha}_2}{9} \frac{\mu R_1 (1 - \rho_1) + \rho_1}{\mu R_1} k_{21} \tilde{g} (1 - \rho_2)^2 (2 + \rho_2) - \frac{\tilde{\alpha}_2}{180} \tilde{g} (3\rho_2^5 - 10\rho_2^3 + 15\rho_2 - 8) \right] \Bigg\}, \quad (120)$$

$$a_{1,0}^{(2)} = -\frac{p}{2G_1}\frac{q_1}{q} + \frac{2}{3}\tilde{\alpha}_1 t_0^{(1)}\left[1 + 2\frac{q_1}{q}(1-\rho_1^3)\right] -$$

$$-G_5\left[\frac{2}{3}\tilde{\alpha}_2 T_0 + \frac{\tilde{\alpha}_2}{9}\frac{\mu R_1(1-\rho_1)+\rho_1}{\mu R_1} k_{21}\tilde{g}(1-\rho_2)^2(2+\rho_2) -\right.$$

$$\left.-\frac{\tilde{\alpha}_2}{180}\tilde{g}(3\rho_2^5 - 10\rho_2^3 + 15\rho_2 - 8)\right]\Bigg\} +$$

$$+\tilde{\alpha}_1 t_0^{(2)}\left[1 + 2\frac{q_1}{q}(\rho_1 - \rho_1^3)\right], \qquad (121)$$

where

$$q = -\frac{(2+2\nu_1)(2-4\nu_2)}{3-3\nu_1}(1-\rho_1^3) -$$

$$-G_{21}\frac{(2+2\nu_2)}{3-3\nu_1}[1+\nu_1+(2-4\nu_1)\rho_1^3],$$

$$q_1 = \frac{(1+\nu_1)(2-4\nu_2) - G_{21}(1+\nu_2)(2-4\nu_1)}{3-3\nu_1},$$

$$q_2 = \frac{2-4\nu_2 + G_{21}(1+\nu_2)}{3-3\nu_1},$$

$$G_6 = \tilde{G}\frac{(2+2\nu_1)}{3-3\nu_1} - 2\left(1 - \tilde{G}\frac{(2-4\nu_1)}{3-3\nu_1}\right)\rho_1^3,$$

$$G_4 = \frac{\tilde{G}}{3-3\nu_1} + \frac{q_2}{q}G_6,\ G_5 = \left(1 - \tilde{G}\frac{(2-4\nu_1)}{3-3\nu_1}\right) + \frac{q_1}{q}G_6,$$

$$\tilde{g} = \frac{R_2^3 g_0}{R_2 - R_3},\ \rho_1 = \frac{R_2}{R_1},\ \rho_2 = \frac{R_3}{R_2},\ k_{21} = \frac{k_2}{k_1}.$$

Thus, the parametric model (107) - (121) is exact, presented in closed form.

9. Computer simulations

This section presents the results of numerical simulation according to the obtained analytical models. Calculations are performed for two types of materials of inclusion and the rest of the ball: stainless steel with thermomechanical characteristics ($G = 80 \cdot 10^9$ Pa, $\nu = 0.28$, $\alpha = 13 \cdot 10^{-6}\,K^{-1}$, $k = 15\,W/(M \cdot K)$, $\sigma = 15\,W/(M^2 K)$) and brass with thermomechanical characteristics ($G = 35.2 \cdot 10^9$ Pa, $\nu = 0.35$, $\alpha = 18.7 \cdot 10^{-6}\,K^{-1}$, $k = 85.5\,W/(M \cdot K)$, $\sigma = 20\,W/(M^2 K)$). Here σ is the heat transfer coefficient, therefore, $\mu = \sigma / k$.

Fixed ball. We will assume that the inclusion material is steel, and the material of the rest of the ball is brass. The problem should not be reduced to a dimensionless form, since for certain values of the parameters, the models considered in the work may go beyond the elastic limits. Since the temperature field in the sphere depends not only on the density of the distributed heat sources, but also on the size of the heat-active region, the radius of the sphere for all the considered cases is fixed and equal to 10^{-1} M. All other sizes are specified in relative form. In this case, the density value can change so that the stresses in the sphere do not exceed the elastic limits of the materials. Further, the ambient temperature T_0 is also recorded at $20^\circ C$ everywhere.

Let us consider the constant density of heat sources of the magnitude $k_2 g_0$, where $g_0 = 10^5 (K/M^2)$. Fig. 1 shows graphs of temperature distribution on the sphere axis depending on the magnitude of the relative shift z_{12} / R_1 of the inclusion center relative to the center of the sphere. It is characteristic that the temperature field remains practically unchanged (the size of the inclusion remains constant $R_2 / R_1 = 0.5$), and only its maximum shifts along with the shift of the inclusion center.

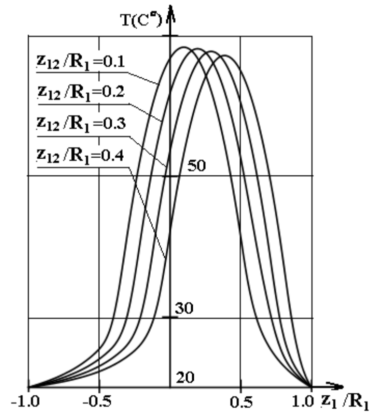

Fig. 1. Temperature distributions on the axis of the ball

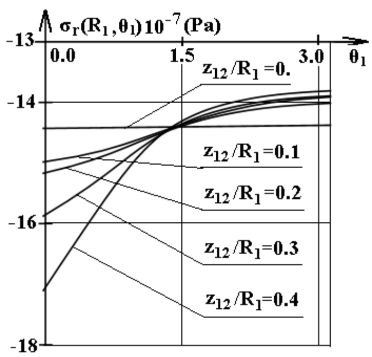

Fig. 2. Distribution of normal stresses on the surface of a ball

Fig. 2 shows the graphs of normal stresses on the surface of the ball. Naturally, their maximum is observed at the upper pole of the sphere – the point that is closest to the heat-active inclusion. As the parameter z_{12} / R_1 decreases, the distribution tends to be uniform.

The case of a concentric inclusion ($z_{12} / R_1 = 0$) is tested on two models. Note that the stresses in the ball do

ISSN 1814-4225 (print)
ISSN 2663-2012 (online)

not go beyond the elastic model, since the proportionality limits for brass and stainless steel are in the range of $190-240\,\text{MPa}$ at a temperature of 50°C, depending on the metal grade.

Fig. 3 shows the temperature distributions on the axis of the sphere depending on the ratio of the radii of the inclusion and the sphere for a fixed value $z_{12} / R_1 = 0.4$ of the relative shift of the centers of the inclusion and the sphere. The density of the heat sources remained unchanged. The nature of the temperature distribution remains practically the same when the parameter R_2 / R_1 changes, only the values of the temperature maxima differ, which mainly depend on the value $g_0 R_2^2$.

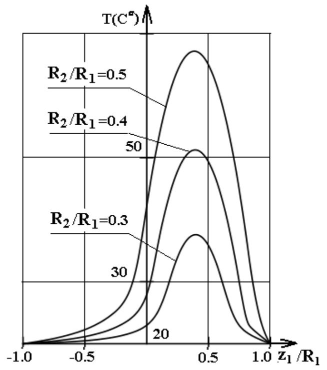

Fig. 3. Temperature distributions on the axis of the ball

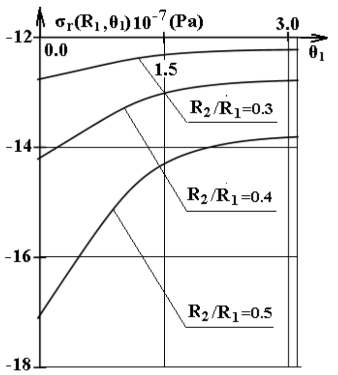

Fig. 4. Distribution of normal stresses
on the surface of a ball

Fig. 4 shows the distributions of normal stresses on the surface of the ball, which correspond to the temperatures given in Fig. 3. As expected, the stresses are compressive, and their maximum absolute values are reached at the upper pole of the sphere. With the specified set of materials for the sphere and inclusion, the above density of the heat sources does not lead to a violation of the elasticity conditions of the model.

The following two figures correspond to the case of linear distribution of the density of heat sources in a heat-active inclusion according to the law

$$g(z_2) = g_0 \left(1 - \frac{z_2}{R_2}\right),$$

where $g_0 = 10^5\,(\text{K}/\text{M}^2)$.

Fig. 5 shows the temperature distribution on the axis of the sphere depending on the relative displacement of the inclusion centers and the sphere at $R_2 / R_1 = 0.5$. A shift in temperature maxima towards the lower pole of the sphere is observed.

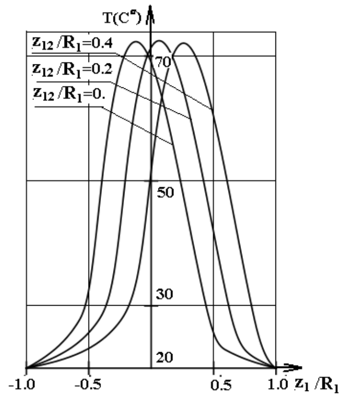

Fig. 5. Temperature distribution on the ball axis

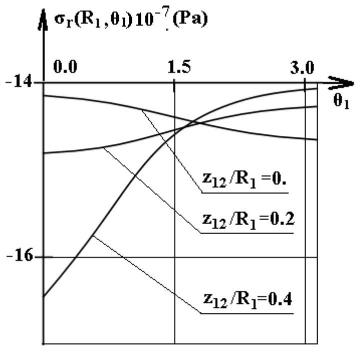

Fig. 6. Distribution of normal stresses
on the surface of a ball

Fig. 6 shows the distribution of normal stresses on the surface of the ball depending on the displacement z_{12} / R_1 of the inclusion center at $R_2 / R_1 = 0.5$. The value $z_{12} / R_1 = 0$ corresponds to a concentric inclusion in a ball. It is interesting that only in this case, of those considered, the decrease in the density of heat sources with an increase in the parameter z_2 / R_2 corresponds to a decrease in tension $\sigma(R_1, \theta_1)$ with an increase in θ_1.

As the graphs in Fig. 7 show, the nature of the temperature distribution has changed somewhat. In addition, it should be taken into account that the value of the constant density of the heat sources was reduced by an order of magnitude ($g_0 = 10^4\,(\text{K}/\text{M}^2)$). However, even with such density, with a sufficiently close location of the inclusion to the boundary of the ball, the stresses in it reach the elastic limit, as it can be seen from Fig. 8.

Loaded ball. The original order of materials is adopted: stainless steel insert, brass ball. The external normal load is considered to be equal to $p = 49.28\,\text{MPa}$. The density of heat sources is considered constant and is determined by the parameter $g_0 = 10^5\,(\text{K}/\text{M}^2)$.

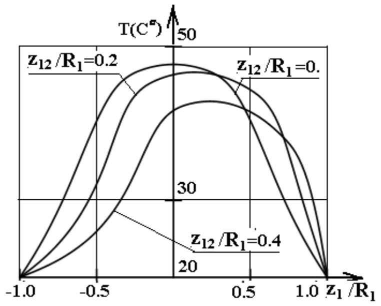

Fig. 7. Temperature distribution on the ball axis

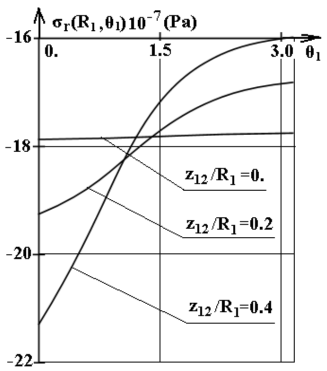

Fig. 8. Distribution of normal stresses on the surface of a ball

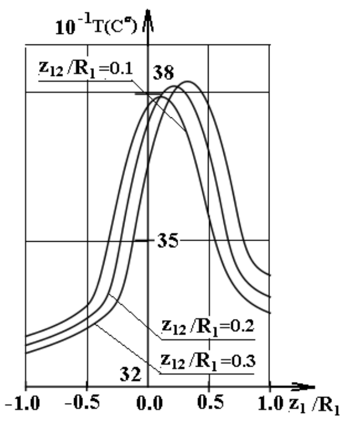

Fig. 9. Temperature distribution on the axis of a loaded ball

To establish the influence of thermomechanical parameters on the nature of the stress-strain state of the ball, the following graphs correspond to a different order of materials: brass for the inclusion and stainless steel for the ball.

The condition of heat exchange of the sphere surface with the environment in the considered model leads to other temperature fields in the sphere. The nature of the distribution and values of temperatures change (Fig. 9). With the above-mentioned density of the heat sources, the temperature in the ball increases by 5-7 times in relation to the fixed model. Now, already at a certain proximity of the inclusion to the surface of the ball, the maximum stresses in it go beyond the elastic model.

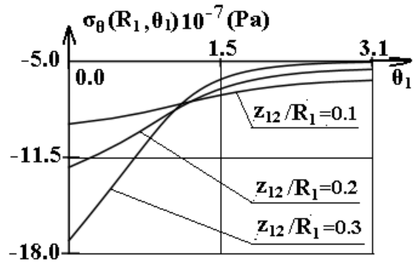

Fig. 10. Distribution of normal angular stresses on the surface of a ball

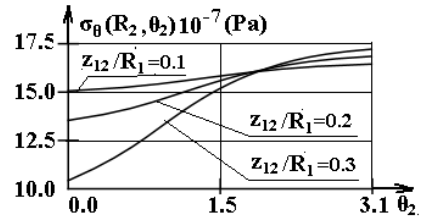

Fig. 11. Distribution of normal angular stresses on the inclusion surface

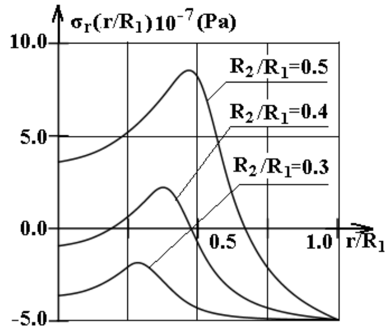

Fig. 12. Distribution of normal radial stresses on the axis of a sphere with a concentric inclusion

Since the normal stresses on the surface of the sphere are determined by the boundary conditions, the graphs of normal angular stresses, which are shown in Fig. 10 for the surface of the sphere and Fig. 11 for the surface of the inclusion, are informative for this model.

ISSN 1814-4225 (print)
ISSN 2663-2012 (online)

Different types of ball and inclusion materials were used in the numerical simulation.

An interesting effect is observed in the model under consideration. Unlike the fixed model, in which the stresses in the sphere were negative for any permissible variations in the parameters, in this model, at a certain density of the heat sources, tensile stresses are observed on the surface of the inclusion (Fig. 11). The reason lies in the significant difference in the thermomechanical parameters of the inclusion and the ball, and at the temperatures shown in Fig. 9, the temperature tensile stresses exceed the mechanical compressive stresses.

Additional confirmation of this conclusion are the graphs of the distribution of normal stresses on the axis of the sphere in the case of concentric inclusions of different radii, shown in Fig. 12.

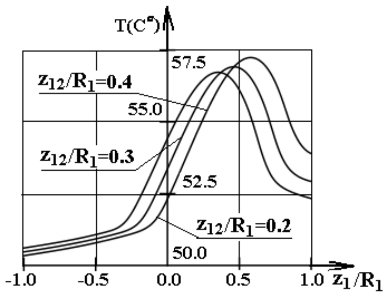

Fig. 13. Temperature distribution on the axis of a loaded sphere

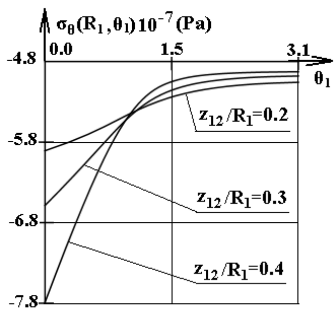

Fig. 14. Distribution of normal angular stresses on the surface of a ball

Fig. 13 and 14 correspond to the case of linear distribution of the density of heat sources in a heat-active inclusion according to the law

$$g(z_2) = g_0\left(1+\frac{z_2}{R_2}\right),$$

where $g_0 = 10^4\ (K/M^2)$. The inclusion material is steel.

The graphs of the change in angular normal stresses are similar to the graphs shown in Fig. 10. The difference in the absolute values of stresses is due to a decrease in the density of heat sources by an order of magnitude. The linear nature of the density has virtually no effect on the distribution of stresses.

We will also present graphs of the temperature distribution (Fig. 15) and normal stresses (Fig. 16) in a ball with a brass inclusion and the linear density of the sources with $g_0 = 10^3 (K/M^2)$.

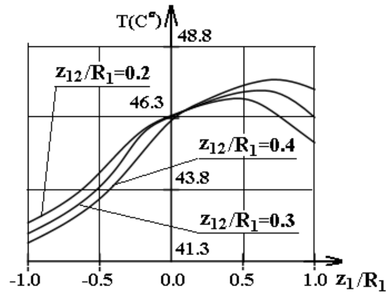

Fig. 15. Temperature distribution on the axis of a ball

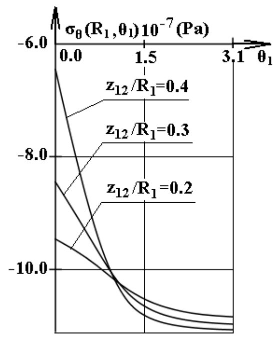

Fig. 16. Distribution of normal angular stresses on the surface of a ball

Note that the nature of the change in temperature and, especially, stress changes significantly compared to the cases considered above. The maximum absolute values of angular compressive stresses are now observed at the lower pole of the sphere (Fig. 16). Of course, this is not only due to the rearrangement of the materials of the sphere and inclusion. For the case under consideration, with an increase in the shear modulus of the material of the ball by 2.27 times, the external normal stress became equal to p = 112 MPa.

Comparison of the graphs shown in Fig. 12 and 17 also shows a different nature of the distribution of normal radial stresses on the axis of the sphere with a concentric inclusion.

Inclusion with a heat-active spherical layer. Let us consider a numerical simulation using the mathematical model from Section 7. A similar model can be used in hyperthermia of deep tissues in the human body in the treatment of tumors using two-phase microparticles: the shell is quartz glass (SiO_2), the core is iron (Fe) [37]. The core performs heating of the particle, and the shell provides biocompatibility, protects the core from oxidation and can perform a number of other functions. The size of these particles can vary from several tens of nanometers to several microns, the heat-active layer is created by Foucault currents, which are generated by an alternating high frequency magnetic field. Since the currents induced by the magnetic field are located in the surface layer of the core with a thickness of $1.0 \cdot 10^{-6} \div 1.5 \cdot 10^{-6}$ M, then when heating nanoparticles, the parametric model of section 6 can be used. For microparticles with a size of $2.0 \cdot 10^{-6} \div 5.0 \cdot 10^{-6}$ M, the model of section 7 works.

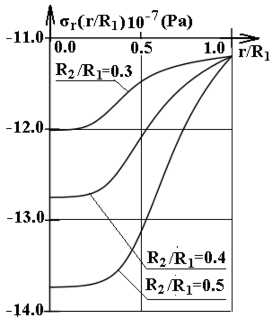

Fig. 17. Distribution of normal radial stresses on the axis of a ball with a concentric inclusion

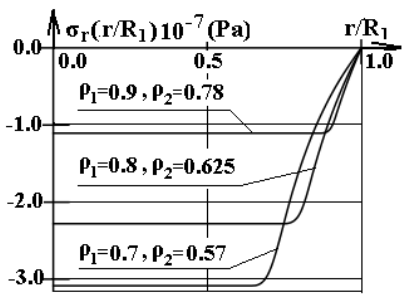

Fig. 18 Distribution of radial stresses along the axis of a spherical particle

The thermomechanical characteristics of the model materials are as follows: for iron ($G_2 = 80 \cdot 10^9$ Pa, $\nu_2 = 0.29$, $\alpha_2 = 12 \cdot 10^{-6}\, K^{-1}$, $k_2 = 75 W/(M \cdot K)$), for quartz glass ($G_1 = 32.0 \cdot 10^9$ Pa, $\nu = 0.18$, $\alpha = 0.5 \cdot 10^{-6}\, K^{-1}$, $k = 1.4 W/(M \cdot K)$, $\sigma = 20 W/(M^2 K)$). The radius of the ball was taken to be $5 \cdot 10^{-6}$ M, the shell thickness varied within $0.5 \cdot 10^{-6} \div 1.5 \cdot 10^{-6}$ M, the thickness of the heat-active layer was $1.0 \cdot 10^{-6} \div 1.5 \cdot 10^{-6}$ M. Blood pressure in muscle tissue was assumed to be $p = 4 \cdot 10^2$ Pa, and its temperature was $36.6^\circ C$.

The density of heat sources was chosen according to formula (106), in which $g_0 = 10^8 K/M^2$. For all the cases considered, a uniform temperature distribution is observed inside the particle at the level $T = 53.4^\circ C$ at $R_2/R_1 = 0.8$, $R_3/R_2 = 0.625$; at the level $T = 51.6^\circ C$ at $R_2/R_1 = 0.9$, $R_3/R_2 = 0.78$; at the level $T = 49.2^\circ C$ at $R_2/R_1 = 0.7$, $R_3/R_2 = 0.57$. The distribution of normal stresses on the particle axis for different thicknesses of the shell and heat-active layer is shown in Fig. 18. The graphs show that the greatest compressive stresses occur in the core and at its boundary with the shell, and among the cases considered - for the shell of greatest thickness. In the region of the core, the stresses remain practically constant.

10. Results and Discussion

Let us summarize the results of the research carried out. The article constructs a number of mathematical models of the axisymmetric stationary thermoelastic state of a ball with a spherical inclusion, provided that the entire inclusion or part of it releases heat according to a harmonic law. The cases of a stationary surface of a sphere with a constant temperature at its boundary, as well as a sphere whose surface is loaded with normal pressure and is in conditions of heat exchange with the environment are considered. It was assumed that the inclusion center was offset from the center of the sphere. The modeling was carried out using the generalized Fourier method, which was further developed in this work. The determination of the parameters of the models was reduced to solving infinite systems of linear algebraic equations, for whose operators the Fredholm property was proven in a certain Hilbert space. For the two specified types of models, the case of a concentric inclusion was considered separately, for which the modeling was carried out using the usual Fourier method. To determine the parameters of the models, linear algebraic systems of the fourth order were obtained. Using a new classical inequality, lower bounds for the moduli of multiparameter determinants of these systems were found for the first time, which made it possible to use the Fourier method to establish the existence classes of the obtained models. A thermoelastic model of a sphere with a heat-active spherical layer in the inclusion was considered separately. The model was found in a closed form. The constructed models were used in a large-scale computer experiment, which considered different types of ball and inclusion materials. Calculations were carried out for temperature fields and stress fields with changes in geometric parameters, values and density functions of heat sources. A wealth of graphic material was obtained and analyzed in the work.

It is important to note that during the calculations, the density of heat sources was controlled, at which the

ISSN 1814-4225 (print)
ISSN 2663-2012 (online)

stresses inside and on the surface of the sphere did not exceed the elastic limit of the constituent materials of the ball. Computer modeling revealed a number of features of the thermoelastic state of the ball. The thermomechanical characteristics of the materials of the outer layer and inclusions have a greater influence on the magnitude of stresses in the ball than on the nature of their distribution. It turned out that the permutation of the materials of the spherical layer and inclusion while maintaining the conditions of elastic deformation leads to the need to reduce the density of heat sources by two orders of magnitude (Fig. 15, 16). In the model of a loaded ball, at certain temperatures and materials of the ball and inclusion, a change in the sign of normal stresses is observed: thermal tensile stresses prevail over mechanical compressive stresses (Fig. 11, 12). The linearity of the heat source distribution density function has little effect on the nature of the temperature and stress distribution in the ball, leading to an additional shift in the maximum of the temperature field along the Oz axis. Modeling of the thermoelastic state of microparticles showed the importance of controlling the density of temperature sources and the geometric sizes of the particles. Calculations have shown that at temperatures $55-70^{\circ}C$ (sometimes used in medicine) and shell thicknesses of 2-2.5 microns, the stresses on the core surface go beyond the elastic limit for quartz glass ($50-70$ MPa). Considering that quartz glass is a brittle material and its elastic limit coincides with its strength limit, preliminary modeling is necessary when designing such particles.

11. Conclusions

Let's draw conclusions based on the research results.

1. The relevance of the research topics is due to the need to model many technical systems with internal heat generation in various areas of human activity.

2. The tasks formulated in section 1.3 of this article to achieve the goal set therein have been achieved.

3. The scientific novelty of the work includes:

– further development of the generalized Fourier method for axisymmetric thermoelastic problems for a ball with an eccentric spherical inclusion;

– construction of mathematical models of the axisymmetric stationary thermoelastic state of a sphere with an eccentric spherical inclusion, provided that the inclusion releases heat according to a harmonic law, and boundary conditions of the first or second kind are satisfied on the surface of the sphere;

– independent construction of the specified models in the case of concentric inclusion;

– construction in closed form of a thermoelastic model of a ball with a heat-active spherical layer in a concentric inclusion;

– the constructed models are strictly justified;

– results of computer modeling based on constructed models for different types of materials of the ball and inclusion, their geometric sizes, values and functions of the density of heat sources, and their analysis.

4. The results obtained in the work have a number of features: the proposed mathematical modeling apparatus is of a universal nature, since it can be applied to multi-connected composite bodies with spherical inclusions; the constructed models analytically accurately satisfy the boundary conditions on the surface of the ball and the conditions for the conjugation of temperature and stress fields on the surface of the inclusion; the models have high computational efficiency, since they require limited (small) computing resources to obtain virtually any predetermined accuracy; the models have a parametric structure and are therefore convenient for use in optimization problems.

5. The reliability of the obtained results is confirmed by the coincidence of independent calculations, which were performed separately for two types of models: exact models with a concentric inclusion and approximately analytical models with an eccentric inclusion with a zero parameter of the shift of the centers of the ball and inclusion.

6. One of the possible practical applications of the obtained models is shown using the example of modeling temperatures and stresses in composite microparticles used in oncology medicine.

Contribution of authors: conceptualization, methodology, formulation of tasks, justification of models, writing – review and editing – **Oleksii Nikolaev**, development of the generalized Fourier method, writing – original draft preparation – **Oleksii Nikolaev, Mariia Skitska,** construction of mathematical models, computer modeling, analysis of results, visualization – **Oleksii Nikolaev, Alina Krainychenko, Mariia Skitska.**

Conflict of Interest

The authors declare that they have no conflict of interest in relation to this research, whether financial, personal, author ship or otherwise, that could affect the research and its results presented in this paper.

Author **Oleksii Nikolaev** is a member of the Editorial Board of this journal. He were not involved in the peer review, handling, or decision-making process for this manuscript.

Financing

This study was conducted without financial support.

Data Availability

The manuscript has no associated data.

Use of Artificial Intelligence

The authors confirm that they did not use artificial intelligence methods while creating the presented work.

Acknowledgments

The authors express their gratitude to Bohdan Drobenko, Doctor of Physical and Mathematical Sciences, Senior Researcher of the Department of Theory of Physical and Mechanical Fields of the Ya. Podstrygach Institute for Applied Problems of Mechanics and Mathematics of the National Academy of Sciences of Ukraine; Tatyana Kagadiy, Doctor of Physical and Mathematical Sciences, Professor, Professor of the Department of Applied Mathematics of the Dnipro Technological University; Natalia Smetankina, Doctor of Technical Sciences, Professor, Head of the Department of Vibration Resistance and Thermal Strength of the A. Podgorny Institute for Problems in Mechanical Engineering of the National Academy of Sciences of Ukraine for discussing some of the results of the work.

All the authors have read and agreed to the published version of this manuscript.

References

1. Lame, M. G. *Lecons Theorie Mathematique. L'elasticitte des corps solides.* Paris: Bachelier, Imprimeur, Libraire, 1852, 335 p. Available at: https://gallica.bnf.fr/ark:/12148/bpt6k5747708p.exteImage (accessed 7 September 2025).

2. Thomson, W. Dynamical problems regarding elastic spheroidal shells and spheroids of incompressible liquid. *Philosophical Transactions of the Royal Society of London,* 1863, vol.153, pp. 583 – 616. DOI: 10.1098/rstl.1863.0028.

3. Somigliana, C. Sopra l'equilibrio di un corpo elastico isotropo limitato da una o due superficie sferiche. *Annali della Scuola Normale Superiore di Pisa, Classe di Scienze,* 1887, S.1, vol. 4, pp. 101-172. Available at: http://www.numdam.org/item?id=ASNSP_1887_1_4__101_0 (accessed 7 September 2025).

4. Cerruti, V. Sulla deformazione di un involucro sferico isotropo per date forze agenti sulle due superficie limiti. *Atti della Reale Accademia dei Lincei, Mem. della Classe di Sc. Fisiche, Matemat'che e Naturali*, 1891, Ser. 4. Annata 287, vol. 7, pp. 25 – 44. DOI: 10.1007/BF02709686.

5. Lure, A. I. *Three-Dimensional Problems of the Theory of Elasticity.* New York: Interscience Publishers, 1964, 493 p. Available at: https://books.google.com.ua/books/about/Three_dimensional_Problems_of_the_Theory.html?id=eUE_AAAAIAAJ &redir_esc=y (accessed 7 September 2025).

6. Strenberg, E., & Rosental, F. The elastic sphere under concentrated loads. *J. Appl. Mech.*, 1952, vol. 19, no. 4, pp. 413 – 424. DOI: 10.1115/1.4010536.

7. Goodier, J.N. Concentration of stress around spherical and cylindrical inclusions and flaws. *ASME J. Appl. Mech.*, 1933, vol.55, no. 7, pp. 39–44. DOI: 10.1115/1.4012173.

8. Amstutz, H., & Vormwald, M. Elastic spherical inhomogeneity in an infinite elastic solid: an exact analysis by an engineering treatment of the problem based on the corresponding cavity solution. *Archive of Applied Mechanics*, 2021, vol. 91, pp. 1577–1603. DOI:10.1007/s00419-020-01842-9.

9. Rahman, M. The stiffness of an elastic solid with an embedded, nominally spherical inclusion subjected to a small arbitrary motion. *International Journal of Solids and Structures*, 2006, vol. 43, pp. 2542–2577. DOI: 10.1016/j.ijsolstr.2005.05.042.

10. Lim, C.W., Li, Z.R., & He, L.H. Size dependent, non-uniform elastic field inside a nano-scale spherical inclusion due to interface stress. *International Journal of Solids and Structures*, 2006, vol. 43, pp. 5055–5065. DOI:10.1016/j.ijsolstr.2005.08.007.

11. Li, Z. R., Lim, C. W., & He, L. H. Stress concentration around a nano-scale spherical cavity in elastic media: effect of surface stress. *European Journal of Mechanics A/Solids*, 2006, vol. 25, pp. 260–270. DOI:10.1016/j.euromechsol.2005.09.005.

12. Zappalorto, M., Salviato, M., & Quaresimin, M. Stress distributions around rigid nanoparticles. *Int J Fract.*, 2012, vol. 176, no. 1, pp. 105-112. DOI:10.1007/s10704-012-9714-2.

13. Nomura, S. Stress fields for a three-phase spherical inclusion problem. *Acta Mech.*, 2021, vol. 232, no. 4, pp. 2843 – 2851. DOI:10.1007/s00707-021-02986-7.

14. Kit, H. S., & Ivas'ko N. M. Two-dimensional problem of thermoelasticity for a half space in the presence of heat release in a ribbon-shaped domain parallel to its boundary. *J. Math. Sci.*, 2019, vol. 236, no. 2, pp. 172–184. DOI:10.1007/s10958-018-4104-6.

15. Meleshko, V. V., Tokovyy, Y., & Barber, G.R. Axially symmetric temperature stresses in an elastic isotropic cylinder of finite length. *J. Math. Sci.*, 2011, vol. 176, no. 5, pp. 646 – 669. DOI:10.1007/s10958-011-0428-1.

16. Protsiuk, B. V. Determination of the Static Thermoelastic State of Layered Thermosensitive Plate, Cylinder, and Sphere. *J. Math. Sci*., 2023, vol. 274, no. 6, pp. 678–707. DOI:10.1007/s10958-023-06630-8.

17. Fesenko, A. A. Mixed Problems of Stationary Heat Conduction and Elasticity Theory for a Semiinfinite Layer. *J Math Sci.*, 2015, vol. 205, pp. 706–718.

ISSN 1814-4225 (print)
ISSN 2663-2012 (online)

DOI: 10.1007/s10958-015-2277-9.

18. Chiang, C. R. Thermal Mismatch Stress of a Spherical Inclusion in a Cubic Crystal. *Int J Fract.*, 2006, vol. 139, no. 2, pp. 313–317. DOI:10.1007/s10704-006-8377-2.

19. Rahman, M., & Michelitsch, T. A general procedure for solving boundary-value problems of elastostatics for a spherical geometry based on Love's approach *Q. J. Mech. Appl. Math.*, 2007, vol. 60. no. 2, pp 139 – 160. DOI:10.1093/qjmam/hbm002.

20. Al-Ali, A. Y., Almutairi, K. H., Rawy, E. K., Ghaleb, A. F., & Abou-Dina, M. S. Deformation of a long thermoelastic rod of rectangular normal cross-section under mixed boundary conditions by boundary integrals. *Journal of the Egyptian Mathematical Society*, 2016, vol. 24, pp. 449–457. DOI: 10.1016/j.joems.2015.09.003.

21. Shiah, Y.C., & Tan, C.L. Thermoelastic analysis of 3D generally anisotropic bodies by the boundary element method. *European Journal of Computational Mechanics*, 2016, vol. 25, no. 1–2, pp. 91–108. DOI:10.1080/17797179.2016.1181038.

22. Hussein, K. Analytical and numerical study of the temperature distribution for a solid sphere subjected to a uniform heat generation. *International Journal of Computer Applications*, 2017, vol. 168, no. 2, pp. 30–37. DOI:10.5120/ijca2017914304.

23. Halazyuk, V.A., & Kit, H.S. Axially symmetric stress-strain state of a body with plane sheet of heat sources. *J. Math. Sci.*, 2012, vol. 183, pp. 162–176. DOI: 10.1007/s10958-012-0804-5.

24. Kit, H. S., & Chernyak, M. S. Stress state of a body with heat-generatingspherical inclusions. *J. Math. Sci.*, 2012, vol. 187, no. 5, pp. 635–646. DOI: https://doi.org/10.1007/s10958-012-1089-4.

25. Kit, H., & Andriychuk, R. Thermal Stressed State of a Half Space with Heat Generation in a Spherical Domain. *J. Math. Sci.*, 2023, vol. 273, no. 1, pp. 1-8. DOI: 10.1007/s10958-023-06488-w.

26. Pawar, S. P., Deshmukh, K. C., & Kedar, G. D. Thermal stresses in functionally graded hollow sphere due to non-uniform internal heat generation. *Applications and Applied Mathematics*, 2015, vol. 10(1), pp. 552 – 569. Available at: https://digitalcommons.pvamu.edu/aam/vol10/iss1/33(accessed 7 September 2025).

27. Rani, P., Singh, K., & Muwal, R. Thermal stresses due to non-uniform internal heat generation in functionally graded hollow cylinder. *Int. J. of Applied Mechanics and Engineering*, 2021, vol.26, no. 2, pp. 186-200. DOI: 10.2478/ijame-2021-0027.

28. Pawar, S. P., Bikram, J. J., & Kedar, G. D. Thermoelastic Behavior in a Multilayer Composite Hollow Sphere with Heat Source. *Journal of Solid Mechanics*, 2020, vol. 12, no. 4, pp. 883–901. DOI: 10.22034/jsm.2020.1898267.1583.

29. Wu, C., & Yin, H. Transient thermal analysis of composites containing spherical inhomogeneities for the particle size effect on laser flash measurements. *Int. J. Solids Struct*. 2025, vol. 321, article no.113540. DOI: 10.1016/j.joems.2015.09.003.

30. Zhang, G., Zhang, Y., Wang, T., Zhang, L., & Gao, Y. Thermoelastic behavior analysis of finite composites embedded in ellipsoidal inhomogeneities with inclusion-based boundary element method. *Int. J. Solids Struct*. 2025, vol. 309, article no.113172. DOI: 10.1016/j.ijsolstr.2024.113172.

31. Rodopoulos, D. C., & Karathanasopoulos, N. Thermomechanical performance of double-phase periodic and graded architected materials: Numerical and explainability analysis. *Int. J. Solids Struct*. 2025, vol. 309, article no. 1131159. DOI: 10.1016/j.ijsolstr.2024.113159.

32. Wang, X., & Schiavone, P. An imperfectly bonded elliptical inhomogeneity under uniform heat flux and uniform temperature change. *Journal of Thermal Stresses.* 2025, vol. 48, is. 4, pp. 458-474. DOI: 10.1080/01495739.2025.2473727.

33. Zeinedini, A. On the role of thermal stress in fracture toughness of polymer nanocomposites: A multiscale theoretical model. *Journal of Thermal Stresses*. 2025, vol. 48, is. 3 Pp. 229-250. DOI: 10.1080/01495739.2025.2473731.

34. Nikolaev, O., & Skitska, M. The method of determining optimal control of the thermoelastic state of piece-homogeneous body using a stationary temperature field. *Radioelectronic and Computer Systems*, 2024, no. 2(110), pp. 98–119. DOI: 10.32620/reks.2024.2.09.

35. Nikolaev, O. G., & Skitska, M. V. Classical problem about an elastic sphere with a spherical inclusion. *Bulletin of the National Technical University "KhPI". Series: Mathematical modeling in engineering and technologies*, 2025, no. 1(8), pp. 107–119. DOI: 10.20998/2222-0631.2025.01(8).13.

36. Buryachenko V. A. *Local and Nonlocal Micromechanics of Heterogeneous Materials*. Springer Nature Switzerland AG, 2022. 999 p. DOI:10.1007/978-3-030-81784-8.

37. Kok, H. P., Cressman, E. N. K, Ceelen, W., Brace, C. L., Ivkov, R., Grüll, H., ter Haar, G., Wust, P., & Crezee, J. Heating technology for malignant tumors: a review. *Int J Hyperthermia*, 2020, vol. 37, no. 1, pp. 711–741. DOI:10.1080/02656736.2020.1779357.

Received 08.09.2025, Received in revised form 12.11.2025
Accepted date 15.01.2026, Published date 22.01.2026

МАТЕМАТИЧНЕ МОДЕЛЮВАННЯ ТЕРМОПРУЖНОГО СТАНУ КУЛИ З ЕКСЦЕНТРИЧНИМ ТЕПЛОАКТИВНИМ СФЕРИЧНИМ ВКЛЮЧЕННЯМ

О. Г. Ніколаєв, А. С. Крайниченко, М. В. Скіцка

Сьогодні технічні системи з внутрішнім тепловиділенням розробляються та використовуються в різних галузях промисловості, енергетики, будівництва, а також у мікроелектроніці, нанотехнологіях, біомедицині, технічній хімії, екології та ін. Створенню подібних систем зазвичай передує їхнє математичне та комп'ютерне моделювання, в якому питання міцності часто відіграють першорядну роль. Використання для цієї мети суто чисельних методів не завжди дає результати потрібної точності, а неможливість параметричного опису моделі не дозволяє вирішувати із нею задач оптимізації. Тому створення нових методів моделювання подібних систем та їх моделей є **актуальною науковою та практичною проблемою**. **Предметом дослідження** цієї статті є математичні моделі термопружного стану кулі зі сферичним включенням, яка має область тепловиділення, а також методи їх отримання. **Метою дослідження** є створення ряду параметричних моделей для дослідження температурних полів та полів напружень у кусково однорідній кулі з внутрішньою теплоактивною областю за різних термомеханічних умов на її межі. Для досягнення поставленої мети **необхідно вирішити низку задач**: виконати подальший розвиток узагальненого методу Фур'є на клас осесиметричних стаціонарних задач термопружності для кулі з ексцентричним теплоактивним сферичним включенням, використовуючи розроблений метод, отримати ряд моделей термопружного стану кулі у випадках ексцентричних та концентричних включень з певною областю тепловиділення в них, виконати строге обґрунтування запропонованого підходу, провести широкий комп'ютерний експеримент з побудованими моделями та виконати аналіз отриманих з його допомогою термомеханічних характеристик, зробити висновки за результатами дослідження. **Методами моделювання** у роботі є узагальнений і звичайний методи Фур'є. У роботі **отримано такі результати**. Побудовано низку математичних моделей осесиметричного стаціонарного термопружного стану кулі зі сферичним включенням за умови, що все включення або його частина виділяє тепло за гармонічним законом. Розглянуто випадки нерухомої поверхні кулі та сталої температури на її межі, а також кулі, поверхня якої навантажена нормальним тиском та знаходиться в умовах теплообміну з навколишнім середовищем. Моделювання проводиться узагальненим методом Фур'є, який у роботі отримав подальший розвиток. Визначення параметрів моделей зводиться до розв'язання нескінченних систем лінійних алгебраїчних рівнянь. Для двох зазначених типів моделей окремо розглядається випадок концентричного включення. Для визначення параметрів моделей отримано лінійні алгебраїчні системи четвертого порядку. З використанням нової класичної нерівності вперше отримано нижні оцінки модулів визначників систем і класи існування одержаних моделей. Окремо в замкненому вигляді отримано термопружну модель кулі зі сферичним теплоактивним шаром у включенні. При чисельному моделюванні використано різні типи матеріалів кулі та включення. Розрахунки проведено для температурних полів та полів напружень при зміні геометричних параметрів, величин та функцій щільності теплових джерел. Отримано багатий графічний матеріал, проаналізований у роботі. **Наукова новизна:** всі перелічені вище результати є новими. Наприкінці зроблено висновки за результатами проведених досліджень.

Ключові слова: математична модель; куля з теплоактивним включенням; узагальнений метод Фур'є; поля температури та напружень; щільність теплових джерел; термомеханічні характеристики; ексцентричне включення; комп'ютерний експеримент; нижня оцінка модуля визначника.

Ніколаєв Олексій Георгійович – д-р фіз.-мат. наук, проф., проф. каф. вищої математики та системного аналізу, Національний аерокосмічний університет «Харківський авіаційний інститут», Харків, Україна.

Крайниченко Аліна Сергіївна – д-р філос., доц. каф. вищої математики та системного аналізу, Національний аерокосмічний університет «Харківський авіаційний інститут», Харків, Україна.

Скіцка Марія Вікторівна – д-р філос., доц. каф. вищої математики та системного аналізу, Національний аерокосмічний університет «Харківський авіаційний інститут», Харків, Україна.

Oleksii Nikolaev – Doctor of Physical and Mathematical Sciences, Professor, Professor at the Department of Higher Mathematics and System Analysis, National Aerospace University "Kharkiv Aviation Institute", Kharkiv, Ukraine,
e-mail: a.nikolaev@khai.edu, ORCID: 0000-0002-7351-1392, Scopus Author ID: 7202396672.

Alina Krainychenko – PhD, Associate Professor at the Department of Higher Mathematics and System Analysis, National Aerospace University "Kharkiv Aviation Institute", Kharkiv, Ukraine,
e-mail: a.krainychenko@khai.edu, ORCID: 0009-0004-5881-4143.

Mariia Skitska – PhD, Associate Professor at the Department of Higher Mathematics and System Analysis, National Aerospace University "Kharkiv Aviation Institute", Kharkiv, Ukraine,
e-mail: m.skitska@khai.edu, ORCID: 0009-0008-8945-6069, Scopus Author ID: 59249590700.